



General Electric Company
178 Turner Avenue, Salt Lake, UT 84120

February 3, 1992

MFN No. 029-92
Docket No. STN 50-605
EEN-9214

Document Control Desk
U.S. Nuclear Regulatory Commission
Washington, D.C. 20555

Attention: Robert C. Pierson, Director
Standardization and Non-Power Reactor Project Directorate

Subject: **Leak Before Break Issue - Decmeber 9-10, 9991 GE/NRC Meeting**

Enclosed are thirty-four (34) copies of the GE response to the subject issue.

It is intended that GE will amend the SSAR with this response in a future amendment.

Sincerely,

R.C. Mitchell, Acting Manager
Regulatory and Analysis Services
M/C 382, (408) 925-6948

cc: F. A. Ross (DOE)
N. D. Fletcher (DOE)
C. Poslusny, Jr. (NRC)
R. C. Berglund (GE)
J. F. Quirk (GE)

Do 28
1/34

ABWR Standard Plant

3.6 PROTECTION AGAINST DYNAMIC EFFECTS ASSOCIATED WITH THE POSTULATED RUPTURE OF PIPING

This Section deals with the structures, systems, components and equipment in the ABWR Standard Nuclear Island.

Subsections 3.6.1 and 3.6.2 describe the design bases and protective measures which ensure that the containment; essential systems, components and equipment; and other essential structures are adequately protected from the consequences associated with a postulated rupture of high-energy piping or crack of moderate-energy piping both inside and outside the containment.

Before delineating the criteria and assumptions used to evaluate the consequences of piping failures inside and outside of containment, it is necessary to define a pipe break event and a postulated piping failure:

Pipe break event: Any single postulated piping failure occurring during normal plant operation and any subsequent piping failure and/or equipment failure that occurs as a direct consequence of the postulated piping failure.

Postulated Piping Failure: Longitudinal or circumferential break or rupture postulated in high-energy fluid system piping or throughwall leakage crack postulated in moderate-energy fluid system piping. The terms used in this definition are explained in Subsection 3.6.2.

Structures, systems, components and equipment that are required to shut down the reactor and mitigate the consequences of a postulated piping failure, without offsite power, are defined as essential and are designed to Seismic Category I requirements.

The dynamic effects that may result from a postulated rupture of high-energy piping include missile generation; pipe whipping; pipe break reaction forces; jet impingement forces; compartment, subcompartment and cavity pressurizations; decompression waves within the ruptured pipes and seven types of loads identified with loss of coolant accident (LOCA) on Table 3.9-2.

23A6100AE

REV. A

Replace

with

Insert A - See p. 3.6-1a

~~Subsection 3.6.3 describes the implementation of the leak-before-break (LBB) evaluation procedures as permitted by the broad scope amendment to General Design Criterion 4 (GDC-4) published in Reference 1. The piping systems that are demonstrated by these procedures to qualify for the LBB behavior (See Appendices 3E and 3F) are not postulated to break in the design and evaluation that are required to be performed, in accordance with Subsections 3.6.1 and 3.6.2, for the potential dynamic effects from postulated piping breaks. However, such piping systems are evaluated for pipe crack effects in accordance with Subsections 3.6.2.1.5 and 3.6.2.1.6.2.~~

3.6.1 Postulated Piping Failures In Fluid Systems Inside and Outside of Containment

This subsection sets forth the design bases, description, and safety evaluation for determining the effects of postulated piping failures in fluid systems both inside and outside the containment, and for including necessary protective measures.

3.6.1.1 Design Bases

3.6.1.1.1 Criteria

Pipe break event protection conforms to 10CFR50 Appendix A, General Design Criterion 4, Environmental and Missile Design Bases. The overall design for this protection is in general compliance with NRC Branch Technical Positions (BTP) ASB 3-1 and MEB 3-1 included in Subsections 3.6.1 and 3.6.2, respectively, of NUREG-0800 (Standard Review Plan).

MEB 3-1 describes an acceptable basis for selecting the design locations and orientations of postulated breaks and cracks in fluid systems piping. Standard Review Plan Sections 3.6.1 and 3.6.2 describe acceptable measures that could be taken for protection against the breaks and cracks and for restraint against pipe whip that may result from breaks.

The design of the containment structure, component arrangement, pipe runs, pipe whip restraints and compartmentalization are done in

Subsection 3.6.3 and Appendix 3E describe the implementation of the leak-before-break (LBB) evaluation procedures as permitted by the broad scope amendment to General Design Criterion 4 (GDC-4) published in Reference 1. It is anticipated, as mentioned in Subsection 3.6.4.2, that a COL applicant will apply to the NRC for approval of LBB qualification of selected piping by submitting a technical justification report. The approved piping, referred to in this SSAR as the LBB-qualified piping, will be excluded from pipe breaks, which are required to be postulated by Subsections 3.6.1 and 3.6.2, for design against their potential dynamic effects. However, such piping are included in postulation of pipe cracks for their effects as described in Subsections 3.6.1.3.1, 3.6.2.1.5 and 3.6.2.1.6.2. It is emphasized that an LBB qualification submittal is not a mandatory requirement; a COL applicant has an option to select from none to all technically feasible piping systems for the benefits of the LBB approach. The decision may be made based upon a cost-benefit evaluation (Reference 6).

standards such as AISC, ACI, and ASME Code Section III, Division II, along with appropriate requirements imposed for similar loading events. These components are also designed for other operational and accident loadings, seismic loadings, wind loadings, and tornado loadings.

The design basis approach of categorizing components is consistent in allowing less stringent inspection requirements for those components subject to lower stresses. Considerable strength margins exist in Type II through IV components up to the limit of load capacity (fracture) of a Type I component. Impact properties in all components are considered since brittle type failures could reduce the restraint system effectiveness.

In addition to the design considerations, strain rate effects and other material property variations have been considered in the design of the pipe whip restraints. The material properties utilized in the design have included one or more of the following methods:

- (1) Code minimum or specification yield and ultimate strength values for the affected components and structures are used for both the dynamic and steady-state events;
- (2) Not more than a 10% increase in minimum code or specification strength values is used when designing components or structures for the dynamic event, and code minimum or specification yield and ultimate strength values are used for the steady-state loads;
- (3) Representative or actual test data values are used in the design of components and structures including justifiably elevated strain rate-affected stress limits in excess of 10%; or
- (4) Representative or actual test data are used for any affected component(s) and the minimum code or specification values are used for the structures for the dynamic and the steady-state events

3.6.2.4 Guard Pipe Assembly Design

The ABWR primary containment does not require guard pipes.

3.6.2.5 Material to be Supplied for the Operating License Review

See Subsection 3.6.4.1

3.6.3 Leak-Before-Break Evaluation Procedures

Per Regulatory Guide 1.70, Revision 3, the safety analysis Section 3.6 has traditionally addressed the protection measures against dynamic effects associated with the non-mechanistic or postulated ruptures of piping. The dynamic effects are defined in introduction to Section 3.6. Three forms of piping failure (full flow area circumferential and longitudinal breaks, and throughwall leakage crack) are postulated in accordance with Subsection 3.6.2 and Branch Technical Position MEB 3-1 of NUREG-0800 (Standard Review Plan) for their dynamic as well as environmental effects.

~~However, in accordance with the revised General Design Criterion 4 (GDC-4) the mechanistic leak-before-break approach (LBB), justified by appropriate fracture mechanics techniques, is now (Reference 1) an acceptable procedure to exclude design against the dynamic effects from the postulation of breaks in high-energy piping. Described in this subsection are the criteria and procedures for the LBB approach which are utilized to qualify piping for exclusion from postulation of breaks. This Subsection is based on proposed (Reference 4) Section 3.6.3 of NUREG-0800.~~

~~The LBB approach is not used to exclude postulation of cracks and associated effects in~~

November 1978,

Replace
with
Insert
A -
see p. 3.6.22

However, in accordance with the modified General Design Criterion 4 (GDC-4), effective November 27, 1987, (Reference 1), the mechanistic leak-before-break (LBB) approach, justified by appropriate fracture mechanics techniques, is recognized as an acceptable procedure under certain conditions to exclude design against the dynamic effects from postulation of breaks in high energy piping. The LBB approach is not used to exclude postulation of cracks and associated effects as required by Subsections 3.6.2.1.5 and 3.6.2.1.6.2. It is anticipated, as mentioned in Subsection 3.6.4.2, that a COL applicant will apply to the NRC for approval of LBB qualification of selected piping. These approved piping, referred to in this SSAR as the LBB-qualified piping, will be excluded from pipe breaks, which are required to be postulated by Subsections 3.6.1 and 3.6.2, for design against their potential dynamic effects.

The following subsections describe (1) certain design bases where the LBB approach is not recognized by the NRC as applicable for exclusion of pipe breaks, and (2) certain conditions which limit the LBB applicability. Appendix 3E provides guidelines for LBB applications describing in detail the following necessary elements of an LBB report to be submitted by a COL applicant for NRC approval: fracture mechanics methods, leak rate prediction methods, leak detection capabilities and typical special considerations for LBB applicability. Also included in Appendix 3E is a list of candidate piping systems for LBB qualification. The LBB application approach described in this subsection and Appendix 3E is consistent with that documented in Draft SRP 3.6.3 (Reference 4) and NUREG-1061 (Reference 5).

ABWR
Standard Plant

23A6100AE
REV. B

~~accordance with Subsections 3.6.2.1.5 and 3.6.2.1.6.2.~~

~~The LBB approach is not applicable to piping systems where operating experience has indicated particular susceptibility to failure from the effects of intergranular stress corrosion cracking (IGSCC), water hammer, thermal fatigues, or erosion.~~

~~The LBB approach is not a replacement for existing regulations or criteria pertaining to the design bases of emergency core cooling system (Subsection 6.3), containment system (Subsection 5.2) or equipment qualification (Subsection 5.11). However, benefits of the LBB procedures to these areas will be taken and the subsections will be revised as the regulations will be relaxed by the NRC. For clarity, it is noted that the LBB approach is not used to relax the design requirements of the primary containment system that includes the primary containment vessel (PCV), vent systems (vertical flow channels and horizontal vent discharges), drywell zones, suppression chamber (wetwell), vacuum breakers, PCV penetrations, and drywell head. However, in designing for loads per Table 3.9-2, which does not apply to these PCV subsystems, the seven types of design loads identified with LOCA-induced dynamics of suppression pool or shield wall annulus pressurization are excluded if they are a result of LOCA postulated in those piping that meet the LBB criteria.~~

Replace with Insert A
See page 3.6-23a

~~Appendix 3E characterizes fracture mechanics properties of piping materials and analysis methods including leakage calculation methods, as required by the criteria of this subsection. Following NRC's review and approval, this appendix will become approved LBB methodology for application to ABWR Standard Plant piping. Appendix 3F applies these properties and methods to specific piping to demonstrate their eligibility for exclusion under the LBB approach. See Subsection 3.6.4.2 for interface requirements.~~

~~3.6.3.1 General Evaluation~~

~~The high-energy piping system (or analyzable~~

Replace with Insert B
Amendment 7
See p. 3.6-23a

~~portion thereof) is evaluated with the following considerations in addition to the deterministic LBB evaluation procedure of Subsection 3.6.3.2~~

- (1) Degradation by erosion, erosion/corrosion and erosion/cavitation due to unfavorable flow conditions and water chemistry is examined. The evaluation is based on the industry experience and guidelines. Additionally, fabrication wall thinning of elbows and other fittings is considered in the purchase specification to assure that the code minimum wall requirements are met. These evaluations demonstrate that these mechanisms are not potential sources of pipe rupture
- (2) The ABWR plant design involves operation below 700°F in ferritic steel piping and below 800°F in austenitic steel piping. This assures that creep and creep-fatigue are not potential sources of pipe rupture.
- (3) The design also assures that the piping material is not susceptible to brittle cleavage-type failure over the full range of system operating temperatures (that is, the material is on the upper shelf).
- (4) The ABWR plant design specifies use of austenitic stainless steel piping made of material (e.g., nuclear grade or low carbon type) that is recognized as resistant to IGSCC. The material of piping in reactor coolant pressure boundary is ferritic steel, except for the austenitic stainless steel reactor water cleanup piping in the primary containment.
- (5) A systems evaluation of potential water hammer is made to assure that pipe rupture due to this mechanism is unlikely. Water hammer is a generic term including various unanticipated high frequency hydrodynamic events such as steam hammer and water slugging. To demonstrate that water hammer is not a significant contributor to pipe rupture, reliance on historical frequency of water hammer events in specific piping systems coupled with a review of operating procedures and conditions is used for this evaluation. The ABWR design includes features such as vacuum breakers and jockey pumps coupled with improved operational procedures to reduce or eliminate the potential for water hammer identified by past

the primary and secondary containments
major high energy
Carbon steel or

3.6.3.1 Scope of LBB Applicability

The LBB approach is not used to replace existing regulations or criteria pertaining to the design bases of emergency core cooling system (Subsection 6.3), containment system (Subsection 6.2) or environmental qualification (Subsection 3.11). However, consistent with modified GDC-4, the design bases for dynamic qualification of mechanical and electrical equipment (Subsection 3.10) may exclude the dynamic load or vibration effects resulting from postulation of breaks in the LBB-qualified piping. This is also reflected in a note to Table 3.9-2 for ASME components. The LBB-qualified piping may not be excluded from the design bases for environmental qualification unless the regulation permits it at the time of LBB qualification. For clarification, it is noted that the LBB approach is not used to relax the design requirements of the primary containment system that includes the primary containment vessel (PCV), vent systems (vertical flow channels and horizontal vent discharges), drywell zones, suppression chamber (wetwell), vacuum breakers, PCV penetrations, and drywell head.

3.6.3.2 Conditions for LBB Applicability

The LBB approach is not applicable to piping systems where operating experience has indicated particular susceptibility to failure from the effects of intergranular stress corrosion cracking (IGSCC), water hammer, thermal fatigue, or erosion. Necessary preventive or mitigation measures are used and necessary analyses are performed, as discussed below, to avoid concerns for these effects. Other concerns, such as creep, brittle cleavage-type failure, potential indirect source of pipe failure, and deviation of as-built piping configuration, are also addressed.

- experience. Certain anticipated water hammer events, such as a closure of a valve, are accounted for in the Code design and analysis of the piping.
- (6) The systems evaluation also addresses a potential for fatigue cracking or failure from thermal and mechanical induced fatigue. Based on past experience, the piping design avoids potential for significant mixing of high- and low- temperature fluids or mechanical vibration. The startup and preoperational monitoring assures avoidance of detrimental mechanical vibration.
- (7) Based on experience and studies by Lawrence Livermore Laboratory, potential indirect sources of indirect pipe rupture are remote causes of pipe rupture. Compliance with the snubber surveillance requirements of the technical specifications assures that snubber failure rates are acceptably low.
- (8) Initial LBB evaluation is based on the design configuration and stress levels that are acceptably higher than those identified by the initial analysis. This evaluation is reconciled when the as-built configuration is documented and the Code stress evaluation is reconciled. It is assured that the as-built configuration does not deviate significantly from the design configuration to invalidate the initial LBB evaluation, or a new evaluation coupled with necessary configuration modifications is made to assure applicability of the LBB procedure.
- (9) ~~Sufficiently reliable, redundant, diverse and sensitive leak detection systems are provided for monitoring of leak. The system that is relied upon to predict the through-wall flaw used in the deterministic fracture mechanics evaluation is sufficiently reliable and sensitive to justify a margin of 2 on the leakage prediction.~~

(1) ~~Use the fracture mechanics and the leak rate computational methods that are accepted by the NRC staff, or are demonstrated accurate with respect to other acceptable computational procedures or with experimental data.~~

(2) ~~Identify the types of materials and materials specifications used for base metal, weldments and safe ends, and provide the materials properties including toughness and tensile data, long-term effects such as thermal aging, and other limitations.~~

(3) ~~Specify the type and magnitude of the loads applied (forces, bending and torsional moments), their source(s) and method of combination. For each pipe size in the functional system, identify the location(s) which have the least favorable combination of stress and material properties for base metal, weldments and safe ends.~~

(4) ~~Postulate a throughwall flaw at the location(s) specified in (3) above. The size of the flaw should be large enough so that the leakage is assured detection with sufficient margin using the installed leak detection capability when the pipes are subjected to normal operating loads. If auxiliary leak detection systems are relied on, they should be described. For the estimation of leakage, the normal operating loads (i.e., deadweight, thermal expansion, and pressure) are to be combined based on the algebraic sum of individual values.~~

~~Using fracture mechanics stability analysis or limit load analysis based on (11) below, and normal plus SSE loads, determine the critical crack size for the postulated throughwall crack. Determine crack size margin by comparing the selected leakage size crack to the critical crack size. Demonstrate that there is a margin of 2 between the leakage and critical crack sizes. The same load combination method selected in (5) below is used to determine the critical crack size.~~

(5) ~~Determine margin in terms of applied loads by a crack stability analysis. Demonstrate~~

3.6.3.2 Deterministic Evaluation Procedure

~~The following deterministic analysis and evaluation are performed as an NRC-approved method for the ABWR Standard Nuclear Island to justify applicability of the LBB concept.~~

Subsection 3.6.3.2 is now Subsection
Amendment 1 3E.1.2 of Appendix 3E
sec. 3E.1-1b

- that the leakage size cracks will not experience unstable crack growth if 1.4 times the normal plus SSE loads are applied. Demonstrate that crack growth is stable and the final crack is limited such that a double-ended pipe break will not occur. The dead-weight, thermal expansion, pressure, SSE (inertial), and seismic anchor motion (SAM) loads are combined based on the same method used for the primary stress evaluation by the ASME Code. The SSE (inertial) and SAM loads are combined by square-root-of-the-sum-of-the-squares (SRSS) method.
- 96) The piping material toughness (J-R curves) and tensile (stress-strain curves) properties are determined at temperatures near the upper range of normal plant operation.
- 97) The specimen used to generate J-R curves is assured large enough to provide crack extensions up to an amount consistent with J/T condition determined by analysis for the application. Because practical specimen size limitations exist, the ability to obtain the desired amount of experimental crack extension may be restricted. In this case, extrapolation techniques is used as described in NUREG-1061, Volume 3, or in NUREG/CR-4575. Other techniques can be used if adequately justified.
- 98) The stress-strain curves are obtained over the range from the proportional limit to maximum load.
- 99) Preferably, the materials tests should be conducted using archival materials for the pipe being evaluated. If archival material is not available, plant specific or industry wide generic material data bases are assembled and used to define the required material tensile and toughness properties. Test material includes base and weld metals.
- 100) To provide an acceptable level of reliability, generic data bases are reasonable lower bounds for compatible sets of material tensile and toughness properties associated with materials at the plant. To assure that the plant-specific generic data base is

adequate, a determination is made to demonstrate that the generic data base represents the range of plant materials to be evaluated. This determination is based on a comparison of the plant material properties identified in (2) above with those of the materials used to develop the generic data base. The number of material heats and weld procedures tested are adequate to cover the strength and toughness range of the actual plant materials. Reasonable lower bound tensile and toughness properties from the plant specific generic data base are to be used for the stability analysis of individual materials, unless otherwise justified.

Industry generic data bases are reviewed to provide a reasonable lower bound for the population of material tensile and toughness properties associated with any individual specification (e.g., A106, Grade B), material type (e.g., austenitic steel) or welding procedures.

The number of material heats and weld procedures tested should be adequate to cover the range of the strength and tensile properties expected for specific material specifications or types. Reasonable lower bound tensile and toughness properties from the industry generic data base are used for the stability analysis of individual materials.

If the data are being developed from an archival heat of material, three stress-strain curves and three J-resistance curves from that one heat of material is sufficient. The tests should be conducted at temperatures near the upper range of normal plant operation. Tests should also be conducted at a lower temperature, which may represent a plant condition (e.g., hot standby) where pipe break would present safety concerns similar to normal operation. These tests are intended only to determine if there is any significant dependence of toughness on temperature over the temperature range of interest. The lower toughness should be used in the fracture mechanics evaluation. One J-R curve and one stress-strain curve for one base metal and weld metal are considered adequate to determine temperature dependence.

(1) There are certain limitations that currently preclude generic use of limit load analyses to evaluate leak-before-break conditions deterministically. However, a modified limit-load analysis can be used for austenitic steel piping to demonstrate acceptable margins as indicated below:

Construct a master Curve where a stress index, SI, given by

$$SI = S + M P_m \quad (1)$$

is plotted as a function of postulated total circumferential throughwall flow length, L, defined by

$$L = 2 \theta R \quad (2)$$

where

$$S = \frac{2 \sigma_f}{\pi} [2 \sin \beta - \sin \theta], \quad (3)$$

$$\beta = 0.5 [(\pi - \theta) - \pi (P_m / \sigma_f)] \quad (4)$$

θ = half angle in radians of the postulated throughwall circumferential flaw.

R = pipe mean radius, that is, the average between the inner and outer radius,

P_m = the combined membrane stress, including pressure, deadweight, and seismic components,

M = 1.4, the margin associated with the load combination method selected for the analysis, per item (5).

σ_f = flow stress for austenitic steel pipe material categories.

If $\theta + \beta$ from Eqs. (2) and (4) is greater than π , then

$$S = \frac{2 \sigma_f}{\pi} \{ \sin \beta \} \quad (5)$$

where

$$\beta = \pi (P_m / \sigma_f) \quad (6)$$

When the master curve is constructed using Eqs. (1), (2), and (3) or (5), the allowable circumferential throughwall flow length can be determined by entering the master curve at a stress index (SI) value determined from the loads and austenitic steel piping material of interest. The allowable flow size determined from the master curve at the appropriate SI value can then be used to determine if the required margins are met. Allowable values of θ are those that result in S being greater than zero from Eqs. (3) and (5). The flow stress used to construct the master curve and the definition of SI used to enter the master curve are defined for each material category as follows:

Base Metal and TIG Welds:

The flow stress used to construct the master curve is

$$\sigma_f = 0.5 (\sigma_y + \sigma_u)$$

when the yield strength, σ_y , and the ultimate strength, σ_u , at temperature are known.

If the yield and ultimate strengths at temperature are not known, then Code minimum values at temperature can be used, or alternatively if

$$(SI) < 2.5, \text{ then } 17M$$

$$\sigma_f = 51 \text{ ksi, or}$$

if

$$(SI) \geq 2.5, \text{ then } 17M$$

$$\sigma_f = 45 \text{ ksi.}$$

The value of SI used to enter the master curve for base metal and TIG welds is

$$SI = M (P_m + P_b) \quad (7)$$

where

P_b = the combined primary bending stress

including deadweight and SSE (inertial) components.

Shielded Metal Arc (SMAW) and Submerged Arc (SAW) Welds:

The flow stress used to construct the master curve is 51 ksi

The value of SI used to enter the master curve for SMAW and SAW is

$$SI = M (P_m + P_b + P_e) Z \quad (8)$$

where

P_b
= the combined primary bending stress, including deadweight and seismic components.

P_e
= combined expansion stress at normal operation.

$$Z = 1.15 [1.0 + 0.013 (OD-4)] \text{ for SMAW,} \quad (9)$$

$$Z = 1.30 [1.0 + 0.010 (OD-4)] \text{ for SAW,} \quad (10)$$

and

OD = pipe outer diameter in inches.

When the allowable flaw length is determined from the master curve at the appropriate SI value, it can be used to determine if the required margins on load and flaw size are met using the following procedure.

For the method of load combination described in item (5), let $M = 1.4$, and if the allowable flaw length from the master curve is at least equal to the leakage size flaw, then the margin on load is met.

3.6.4 Interfaces

3.6.4.1 Details of Pipe Break Analysis Results and Protection Methods

The following shall be provided by the applicant ~~referencing the ABWR design~~ (See Subsection 3.6.2.5):

(1) A summary of the dynamic analyses applicable to high-energy piping systems in accordance with Subsection 3.6.2.5 of Regulatory Guide 1.70. This shall include:

(a)

Sketches of applicable piping systems showing the location, size and orientation of postulated pipe breaks and the location of pipe whip restraints and jet impingement barriers.

(b)

A summary of the data developed to select postulated break locations including calculated stress intensities, cumulative usage factors and stress ranges as delineated in BTP MEB 3-1.

(2) For failure in the moderate-energy piping systems listed in Table 3.6-6, descriptions showing how safety-related systems are protected from the resulting jets, flooding and other adverse environmental effects.

(3) Identification of protective measures provided against the effects of postulated pipe failures in each of the systems listed in Tables 3.6-1, 3.6-2, and 3.6-4.

(4) The details of how the MSIV functional capability is protected against the effects of postulated pipe failures.

(5) Typical examples, if any, where protection for safety-related systems and components against the dynamic effects of pipe failures include their enclosure in suitably designed structures or compartments (including any additional drainage system or equipment environmental qualification needs).

(6) The details of how the feedwater line check and feedwater isolation valves functional capabilities are protected against the effects of postulated pipe failures.

3.6.4.2 Leak-Before-Break Analysis Report

As required by Reference 1, an LBB analysis

410.21
410.22
410.26
410.28

COL
^

report shall be prepared for the piping systems proposed for ~~inclusion~~^{exclusion} from the analyses for the dynamic effects due to their failure. The report shall include ~~only the piping stress analysis results for the piping systems analyzed and reported for LBB in Appendix 3F in order to show that the piping stresses are within the stress levels assumed in Appendix 3F (See Subsection 3.6.3).~~

be prepared in accordance with the guidelines presented in Appendix 3E and submitted by the col applicant to the NRC for approval.

3.6.5 References

1. *Modification of General Design Criterion 4 Requirements for Protection Against Dynamic Effects of Postulated Pipe Rupture*, Federal Register, Volume 52, No. 207, Rules and Regulations, Pages 41288 to 41295, October 27, 1987
2. *RELAP 3, A Computer Program for Reactor Blowdown Analysis*, IN-1321, issued June 1970, Reactor Technology TID-4500.
3. Moody, F. J., *Fluid Reactor and Impingement Loads*, Vol. 1, ASCE Specialty Conference on Structural Design of Nuclear Plant Facilities pp. 219-262, December 1973.
4. *Standard Review Plan; Public Comments Solicited*, Federal Register, Volume 52, No. 167, Notices, Pages 32626 to 32633, August 28, 1987.
5. NUREG-1061, Volume 3, Evaluation of Potential for Pipe Breaks, Report of the U.S. NRC Piping Review Committee, November 1984.
6. Mehta, H.S., Patel, N.T. and Ranganath, S., "Application of the Leak-Before-Break Approach to BWR Piping," Report NP-4991, Electric Power Research Institute, Palo Alto, Ca, December 1986.

APPENDIX 3E

GUIDELINES FOR LBB APPLICATIONS

APPENDIX 3E
TABLE OF CONTENTS

Section	Title	Page
3E	<u>GUIDELINES FOR LBB APPLICATIONS</u> <u>FRACTURE MECHANICS, LEAK RATE</u> <u>CALCULATION AND LEAK DETECTION</u> <u>METHODS</u>	
3E.1	<u>INTRODUCTION</u>	3E.1-1
3E.2	<u>MATERIAL FRACTURE TOUGHNESS</u> <u>CHARACTERIZATION</u>	3E.2-1
3E.2.1	Fracture Toughness Characterization	3E.2-1
3E.2.2	Carbon Steels and Associated Welds	3E.2-2
3E.2.3	References	3E.2-5
3E.3	<u>FRACTURE MECHANIC METHODS</u>	3E.3-1
3E.3.1	Elastic Plastic Fracture Mechanics or (J/T) Methodology	3E.3-1
3E.3.2	Application of (J/T) Methodology to Carbon Steel Piping	3E.3-3
3E.3.3	References	3E.3-3
3E.4	<u>LEAK RATE CALCULATION METHODS</u>	3E.4-1
3E.4.1	Leak Rate Estimation for Pipes Carrying Water	3E.4-1
3E.4.2	Flow Rate Estimation for Saturated Steam	3E.4-2
3E.4.3	References	3E.4-4
3E.5	<u>LEAK DETECTION CAPABILITIES</u>	3E.5-1
3E.6	<u>GUIDELINES FOR PREPARATION</u> <u>OF AN LBB REPORT</u>	
3E.6.1	Main Steam Piping Example	3E.6-1
3E.6.2	Feed Water Piping Example	
	3E-ii	
3E.1.1	Material Selection Guidelines	3E.1-1b
3E.1.2	Deterministic Evaluation Procedure	3E.1-1c

SECTION 3E.1

CONTENTS

<u>Section</u>	<u>Title</u>	<u>Page</u>
3E.1.1	Material Selection Guidelines	3E.1-1b
3E.1.2	Deterministic Evaluation Procedure	3E.1-1c

TABLES

<u>Table</u>	<u>Title</u>	<u>Page</u>
3E.1-1	Leak Before Break Candidate Piping Piping Systems	3E.1-1f

APPENDIX 3E
GUIDELINES FOR LBB APPLICATIONS
~~FRACTURE MECHANICS, LEAK RATE CALCULATION
AND LEAK DETECTION METHODS~~

3E.1 INTRODUCTION

Insert A see p. 3E.1-1 a

As discussed in Subsection 3.6.3, this appendix characterizes the fracture mechanics properties of ABWR piping materials and analysis methods, including the leak rate calculation methods. ~~In Appendix 3E, these properties and methods are applied to specific piping systems to demonstrate their eligibility for the LBB qualification.~~ Insert B see p. 3E.1-1 a

Piping qualified by LBB would be excluded from the non-mechanistic postulation requirements of double-ended guillotine break (DEGB) specified in Subsection 3.6.3. The LBB qualification means that the through-wall flaw lengths that are detectable by leakage monitoring systems (see Subsection 5.2.5) are significantly smaller than the flaw lengths that could lead to pipe rupture or instability.

Section 3E.2 addresses the fracture mechanics properties aspects required for evaluation in accordance with Subsection 3.6.3. Section 3E.3 describes the fracture mechanics techniques and methods for the determination of critical flaw lengths and evaluation of flaw stability. Explained in Section 3E.4 is the determination of flaw lengths for detectable leakages with margin. ~~Finally,~~ ^A brief discussion on the leak detection capabilities is presented in Section 3E.5. Insert C see p. 3E.1-1b thru c

INSERTS FOR PAGE 3E.1-1

Insert A

..provides detailed guidelines for applicant's use in applying for NRC's approval of LBB for specific piping systems. Also included in this appendix are ..

Insert B

Table 3E.1-1 gives a list of piping systems inside and outside the containment that are preliminary candidates for LBB application. As noted on Table 3E.1-1, most candidate piping systems are carbon steel piping. Therefore, this appendix deals extensively with the evaluation of carbon steel piping.

Insert G

Finally, Section 3E.6 provides general guidelines for the preparation of LBB justification reports by providing two examples.

Material selection and the deterministic LBB evaluation procedure are discussed in this section.

3E.1.1 Material Selection Guidelines

The LBB approach is applicable to piping systems for which the materials meet the following criteria: (1) low probability of failure from the effects of corrosion (e.g., intergranular stress corrosion cracking) and (2) adequate margin before susceptibility to cleavage type fracture over the full range of systems operating temperatures where pipe rupture could have significant consequences.

The ABWR plant design specifies use of austenitic stainless steel piping made of material (e.g., nuclear grade or low carbon type) that is recognized as resistant to IGSCC. The carbon steel or ferritic steels specified for the reactor pressure boundary are described in 3E.2.2. These steels are assured to have adequate toughness to preclude a fracture at operating temperatures. A COL applicant is expected to supply a detailed justification in the LBB evaluation report considering system temperature, fluid velocity and environmental conditions.

3E.1.2 Deterministic Evaluation Procedure

The following deterministic analysis and evaluation are performed as an NRC-approved method ~~for the ABWR Standard Nuclear Island~~ to justify applicability of the LBB concept.

- (1) Use the fracture mechanics and the leak rate computational methods that are accepted by the NRC staff, or are demonstrated accurate with respect to other acceptable computational procedures or with experimental data.
- (2) Identify the types of materials and materials specifications used for base metal, weldments and safe ends, and provide the materials properties including toughness and tensile data, long-term effects such as thermal aging, and other limitations.
- (3) Specify the type and magnitude of the loads applied (forces, bending and torsional moments), their source(s) and method of combination. For each pipe size in the functional system, identify the location(s) which have the least favorable combination of stress and material properties for base metal, weldments and safe ends.
- (4) Postulate a throughwall flaw at the location(s) specified in (3) above. The size of the flaw should be large enough so that the leakage is assured detection with sufficient margin using the installed leak detection capability when the pipes are subjected to normal operating loads. If auxiliary leak detection systems are relied on, they should be described. For the estimation of leakage, the normal operating loads (i.e., deadweight, thermal expansion, and pressure) are to be combined based on the algebraic sum of individual values.

Using fracture mechanics stability analysis or limit load analysis based ~~on (ii) below~~ ^{← stat} and normal plus SSE loads, determine the critical crack size for the postulated throughwall crack. Determine crack size margin by comparing the selected leakage size crack to the critical crack size. Demonstrate that there is a margin of 2 between the leakage and critical crack sizes. The same load combination method selected in (5) below is used to determine the critical crack size.

- (5) Determine margin in terms of applied loads by a crack stability analysis. Demonstrate

that the leakage size cracks will not experience unstable crack growth if 1.4 times the normal plus SSE loads are applied. Demonstrate that crack growth is stable and the final crack is limited such that a double-ended pipe break will not occur. The dead-weight, thermal expansion, pressure, SSE (inertial), and seismic anchor motion (SAM) loads are combined based on the same method used for the primary stress evaluation by the ASME Code. The SSE (inertial) and SAM loads are combined by square-root-of-the-sum-of-the-squares (SRSS) method.

- (6) The piping material toughness (J-R curves) and tensile (stress-strain curves) properties are determined at temperatures near the upper range of normal plant operation.
- (7) The specimen used to generate J-R curves is assured large enough to provide crack extensions up to an amount consistent with J/T condition determined by analysis for the application. Because practical specimen size limitations exist, the ability to obtain the desired amount of experimental crack extension may be restricted. In this case, extrapolation techniques is used as described in NUREG-1061, Volume 3, or in NUREG/CR-4575. Other techniques can be used if adequately justified.
- (8) The stress-strain curves are obtained over the range from the proportional limit to maximum load.
- (9) Preferably, the materials tests should be conducted using archival materials for the pipe being evaluated. If archival material is not available, plant specific or industry wide generic material data bases are assembled and used to define the required material tensile and toughness properties. Test material includes base and weld metals.
- (10) To provide an acceptable level of reliability, generic data bases are reasonable lower bounds for compatible sets of material tensile and toughness properties associated with materials at the plant. To assure that the plant specific generic data base is

adequate, a determination is made to demonstrate that the generic data base represents the range of plant materials to be evaluated. This determination is based on a comparison of the plant material properties identified in (2) above with those of the materials used to develop the generic data base. The number of material heats and weld procedures tested are adequate to cover the strength and toughness range of the actual plant materials. Reasonable lower bound tensile and toughness properties from the plant specific generic data base are to be used for the stability analysis of individual materials, unless otherwise justified.

Industry generic data bases are reviewed to provide a reasonable lower bound for the population of material tensile and toughness properties associated with any individual specification (e.g., A106, Grade B), material type (e.g., austenitic steel) or welding procedures.

The number of material heats and weld procedures tested should be adequate to cover the range of the strength and tensile properties expected for specific material specifications or types. Reasonable lower bound tensile and toughness properties from the industry generic data base are used for the stability analysis of individual materials.

If the data are being developed from an archival heat of material, three stress-strain curves and three J-resistance curves from that one heat of material is sufficient. The tests should be conducted at temperatures near the upper range of normal plant operation. Tests should also be conducted at a lower temperature, which may represent a plant condition (e.g., hot standby) where pipe break would present safety concerns similar to normal operation. These tests are intended only to determine if there is any significant dependence of toughness on temperature over the temperature range of interest. The lower toughness should be used in the fracture mechanics evaluation. One J-R curve and one stress-strain curve for one base metal and weld metal are considered adequate to determine temperature dependence.

- continued next page -

(11) There are certain limitations that currently preclude generic use of limit load analyses to evaluate leak-before-break conditions deterministically. However, a modified limit-load analysis can be used for austenitic steel piping to demonstrate acceptable margins as described in 3E.3.3.

TABLE 3E.1-1

LEAK BEFORE BREAK CANDIDATE
PIPING SYSTEMS

System	Location	Description	Diameter (mm)
Main Steam (4 Lines)	PC	RPV to RCCV	700
Feedwater (2 Lines/6 Risers)	PC	RPV to RCCV	550/300
RCIC Steam	PC	MS to RCCV	150
HPCF	PC	RPV to first check valve	200
RHR/LPFL	PC	RPV to first check valve	250
RHR Suction	PC	RPV to first closed gate valve	350
CUW	PC	RHR suction to RCCV	200
Main Steam (4 Lines)	Steam Tunnel	RCCV to turbine building	700
Feedwater (2 Lines)	Steam Tunnel	RCCV to turbine building	550
RHR Div. A Suction	Steam Tunnel	FW line A to check valve	250
RCIC Steam	SC	RCCV to turbine shutoff valve	150
RCIC Supply	SC	FW to first check valve	200
CUW Suction	SC	RCCV to heat exchanger discharge	200
CUW Discharge	SC	Heat exchanger discharge to FW suction	200/150

Note: (1) All piping in primary and secondary containment (including steam tunnel) are carbon steel piping, except the in-containment CUW piping which is stainless steel.

Legend: PC: Primary Containment
SC: Secondary Containment
FW: Feedwater

SECTION 3E.2
CONTENTS

Section	Title	Page
3E.2.1	<u>Fracture Toughness Characterization</u>	3E.2-1
3E.2.2	<u>Carbon Steels and Associated Welds</u>	3E.2-2
3E.2.2.1	Fracture Toughness Test Program	3E.2-2
3E.2.2.1.1	Charpy Tests	3E.2-3
3E.2.2.1.2	Stress-Strain Tests	3E.2-3
3E.2.2.1.3	J-R Curve Tests	3E.2-4
3E.2.2.2	Material (J/T) Curve Selection	3E.2-4
3E.2.2.2.1	Material (J/T) Curve for 550° F	3E.2-4
3E.2.2.2.2	Material (J/T) Curve for 420° F	3E.2-5
3E.2.3	<u>Stainless Steels and Associated Welds</u>	3E.2-5 a
3E.2.3.4	<u>References</u>	3E.2-5

TABLES

Table	Title	Page
3E.2-1	Electrodes and Filler Metal Requirements for Carbon Steel Welds	3E.2-7
3E.2-2	Supplier Provided Chemical Composition and Mechanical Properties Information	3E.2-8
3E.2-3	Standard Tension Test Data At Temperature	3E.2-9
3E.2-4	Summary of Carbon Steel J-R Curve Tests	3E.2-10

SECTION 3E.2
ILLUSTRATIONS

Figure	Title	Page
3E.2-1a	Schematic Representation of Material J-Integral R Curve	3E.2-11
3E.2-1b	Schematic Representation of Material J-T Curve	3E.2-11
3E.2-2	Carbon Steel Test Specimen Orientation Code	3E.2-12
3E.2-3	Toughness Anisotropy of ASTM 106 Pipe (6 in Sch. 80)	3E.2-13
3E.2-4a	Charpy Energies for Pipe Test Material as a Function of Orientation and Temperature	3E.2-14
3E.2-4b	Charpy Energies for Plate Test Material as a Function of Orientation and Temperature	3E.2-15
3E.2-5	Comparison of Base Metal, Weld and HAZ Charpy Energies for SA333 GR. 6	3E.2-16
3E.2-6a	Plot of 550 ^o F True Stress-True Strain Curves for SA333 GR. 6 Carbon Steel	3E.2-17
3E.2-6b	Plot of 550 ^o F True Stress-True Strain Curves for SA516 GR. 70 Carbon Steel	3E.2-18
3E.2-6c	Plot of 350 ^o F True Stress-True Strain Curves for SA333 Gr. 6 Carbon Steel	3E.2-19
3E.2-6d	Plot of 350 ^o F True Stress-True Strain Curves for SA516 Gr. 70 Carbon Steel	3E.2-20
3E.2-7	Plot of 550 ^o F Test J-R Curve for Pipe Weld	3E.2-21
3E.2-8	Plot of 550 ^o F J _{mod} , T _{mod} Data From Test J-R Curve	3E.2-22
3E.2-9	Carbon Steel J-T Curve for 420 ^o F	3E.2-23

3E.2 MATERIAL FRACTURE TOUGHNESS CHARACTERIZATION

This subsection describes the fracture toughness properties and flow stress evaluation for the ferritic materials used in ABWR plant piping, as required for evaluation according to Section 3E.1.2.

3E.2.1 Fracture Toughness Characterization

When the elastic-plastic fracture mechanics (EPFM) methodology or the J-T methodology is used to evaluate the leak-before-break conditions with postulated through-wall flaws, the material toughness property is characterized in the form of J-integral resistance curve (or J-R curve) [1, 2, 3]. The J-R curve, schematically shown in Figure 3E.2-1a, represents the material's resistance to crack extension. The onset of crack extension is assumed to occur at a critical value of J. Where the plane strain conditions are satisfied, initiation J is denoted by J_{IC} . Plane strain crack conditions, achieved in test specimen by side grooving, generally provide a lower bound behavior for material resistance to stable crack growth.

Once the crack begins to extend, the increase of J with crack growth is measured in terms of slope or the nondimensional tearing modulus, T, expressed as:

$$T = \frac{E}{\sigma_f^2} \cdot \frac{dJ}{da} \quad (E.2-1)$$

The flow stress, σ_f , is a function of the yield and ultimate strength, and E is the elastic modulus. Generally, σ_f is assumed as the average of the yield and ultimate strength. The slope $\frac{dJ}{da}$ of the material J-R curve is a function of crack extension Δa . Generally, $\frac{dJ}{da}$ decreases with crack extension thereby giving a convex upward appearance to the material J-R curve in Figure 3E.2-1a.

To evaluate the stability of crack growth, it is convenient to represent the material J-R curve in the J-T space as shown in Figure 3E.2-1b. The resulting curve is labeled as J-T material. Crack instability is predicted at the intersection point of the J/T material and J/T applied curves.

The crack growth invariably involves some elastic unloading and distinctly nonproportional plastic deformation near the crack tip. J-integral is based on the deformation theory of plasticity [4, 5] which inadequately models both of these aspects of plastic behavior. In order to use J-integral to characterize crack growth (i.e. to assure J-controlled crack growth), the following sufficiency condition in terms of a nondimensional parameter proposed by Hutchinson and Paris [6], is used:

$$\omega = \frac{b}{J} \cdot \frac{dJ}{da} \gg 1 \quad (E.2-2)$$

Where b is the remaining ligament. Reference 7 suggests that $\omega > 10$ would satisfy the J-controlled growth requirements. However, if the requirements of this criteria are strictly followed, the amount of crack growth allowed would be very small in most test specimen geometries. Use of such a material J-R curve in J/T evaluation would result in grossly underpredicting the instability loads for large diameter pipes where considerable stable crack growth is expected to occur before reaching the instability point. To overcome this difficulty, Ernst [8] proposed a modified J-integral, J_{mod} , which was shown to be effective even when limits on ω were grossly violated. The Ernst correction essentially factors-in the effect of crack extension in the calculated value of J. This correction can be determined experimentally by measuring the usual parameters: load, displacement and crack length.

The definition of J_{mod} is:

$$J_{mod} = J + \int_{a_0}^a \frac{\partial(J-G)}{\partial a} \delta_{pl} da \quad (E.2-3)$$

Where

J is based on deformation theory of plasticity

G is the linear elastic Griffith energy release rate or elastic J, J_{el} .

δ_{pl} is the nonlinear part of the load-point displacement, (or simply the total minus the elastic

displacement).

a_0, a are the initial and current crack lengths respectively.

For the particular case of the compact tension specimen geometry, the preceding Equation and the corresponding rate take the form

$$J_{mod} = J + \int_{a_0}^a \gamma \cdot \frac{J_{pl}}{b} da \quad (E.2-4)$$

where J_{pl} is the nonlinear part of the deformation theory J , b is the remaining ligament and γ is

$$\gamma = (1 + 0.76 b/W) \quad (E.2-5)$$

Consequently the modified material tearing modulus T_{mod} can be defined as:

$$T_{mod} = T_{mat} + \frac{E}{\sigma_f^2} \frac{\gamma \cdot J_{pl}}{b} \quad (E.2-6)$$

Since in most of the test J-R curves the $\omega > 10$ limit was violated, all of the material J-T data were recalculated in the J_{mod}, T_{mod} format. The J_{mod}, T_{mod} calculations were performed up to crack extension of $\Delta a = 10\%$ of the original ligament in the test specimen. The J-T curves were then extrapolated to larger J values using the method recommended in NUREG 1061, Vol. 3 [9].

3E.2.2 Carbon Steels and Associated Welds

The carbon steels used in the ABWR reactor coolant pressure boundary piping are: SA 106 Gr B, SA 333 Gr. 6 and SA 672, Gr. C70. The first specification covers seamless pipe and the second one pertains to both seamless and seam-welded pipe. The last one pertains to seam-welded pipe for which plate stock is specified as SA 516, Gr. 70. The corresponding material specifications are given by a GE specification [10] equivalent to the piping specifications.

While the chemical composition requirements for a pipe per SA 106 Gr. B and SA 333 Gr. 6 are identical, the latter is subjected to two additional requirements: (1) a normalizing heat

treatment which refines the grain structure and, (2) a Charpy test at -50°F with a specified minimum absorbed energy of 13 ft-lbs.

The electrodes and filler metal requirements for welding carbon steel to carbon or low alloy steel are as specified in Table 3E.2-1. A comprehensive test program was undertaken to characterize the carbon steel base and weld material toughness properties. The next section describes the scope and the results of this program.

3E.2.2.1 Fracture Toughness Test Program

The test program consisted of generating true stress-true strain curves, J-Resistance curves and the Charpy V-notch tests. Two materials were selected: (1) SA333 Gr. 6, 16 inch diameter Schedule 80 pipe and (2) SA516, Gr. 70, 1 1/4 inch thickness plate. Table 3E.2-2 shows the chemical composition and mechanical property test information provided by the material supplier. The materials were purchased to the same specifications as those to be used in the ABWR applications.

To produce a circumferential butt weld, the pipe was cut in two pieces along a circumferential plane and welded back using the shielded metal arc process. The weld prep was of single V design with a backing ring. The preheat temperature was 200°F .

The plate material was cut along the longitudinal axis and welded back using the SAW process. The weld prep was of a single V type with one side as vertical and the other side at 45° . A backing plate was used during the welding with a clearance of 1/4 inch at the bottom of the V. The interpass temperature was maintained at less than 500°F .

Both the plate and the pipe welds were X-rayed according to Code [11] requirements and were found to be satisfactory.

It is well-known that carbon steel base materials show considerable anisotropy in fracture toughness properties. The toughness depends on the orientation and direction of propagation of the crack in relation to the principal direction of mechanical working or

grain flow. Thus, the selection of proper orientation of Charpy and J-R curve test specimen is important. Figure 3E.2-2 shows the orientation code for rolled plate and pipe specimen as given in ASTM Standard E399 [12]. Since a through-wall circumferential crack configuration is of most interest from the DEGB point of view, the L-T specimen in a plate and the L-C specimen in a pipe provide the appropriate toughness properties for that case. On the other hand, T-L and C-L specimen are appropriate for the axial flaw case.

Charpy test data are reviewed first since they provide a qualitative measure of the fracture toughness.

3E.2.2.1.1 Charpy Tests

The absorbed energy or its complement, the lateral expansion measured during a Charpy V-notch test provides a qualitative measure of the material toughness. For example, in the case of austenitic stainless steel flux weldments, the observed lower Charpy energy relative to the base metal was consistent with the similar trend observed in the J-Resistance curves. The Charpy tests in this program were used as preliminary indicators of relative toughness of welds, HAZs and the base metal.

The carbon steel base materials exhibit considerable anisotropy in the Charpy energy as illustrated by Figure 3E.2-3 from Reference 13. This anisotropy is associated with development of grain flow due to mechanical working. The Charpy orientation C in Figure 3E.2-3 (orientations LC and LT in Figure 3E.2-2) is the appropriate one for evaluating the fracture resistance to the extension of a through-wall circumferential flaw. The upper shelf Charpy energy associated with axial flaw extension (orientation A in Figure 3E.2-3) is considerably lower than that for the circumferential crack extension.

A similar trend in the base metal Charpy energies was also noted in this test program. Figures 3E.2-4a and b show the pipe and plate material Charpy energies for the two orientations as a function of temperature. The tests were conducted at six temperatures ranging from room temperature to 550° F. From the trend of the Charpy energies as a function of temperature in

Figures 3E.2-4a and b it is clear that even at room temperature the upper shelf conditions have been reached for both the materials.

No such anisotropy is expected in the weld metal since it does not undergo any mechanical working after its deposition. This conclusion is also supported by the available data in the technical literature. The weld metal Charpy specimen in this test program were oriented the same way as the LC or LT orientations in Figure 3E.2-2. The HAZ Charpy specimens were also oriented similarly.

Figure 3E.2-5 shows a comparison of the Charpy energies from the 333 Gr. 6 base metal, the weld metal and the HAZ. In most cases two specimens were used. Considerable scatter in the weld and HAZ Charpy energy values is seen. Nevertheless, the average energies from the weld metal and the HAZ seem to fall at or above the average base metal values. This indicates that, unlike the stainless steel flux weldments, the fracture toughness of carbon steel weld and HAZ, as measured by the Charpy tests, is at least equal to the carbon steel base metal.

The preceding results and the results of the stress-strain tests discussed in the next section were used as a basis to choose between the base and the weld metal properties for use in the J-T methodology evaluation.

or other similar etc

3E.2.2.1.2 Stress-Strain Tests

The stress-strain tests were performed at three temperatures: Room temperature, 350° F and 550° F. Base and weld metal from both the pipe and the plate were tested. The weld specimens were in the as-welded condition. The standard test data obtained from these tests are summarized in Table 3E.2-3.

An examination of Table 3E.2-3 shows that the measured yield strength of the weld metal, as expected, is considerably higher than that of the base metal. For example, the 550° F yield strength of the weld metal in Table 3E.2-3 ranges from 53 to 59 ksi, whereas the base metal yield strength is only 34 ksi. The impact of this observation in the selection of appropriate material (J/T) curve is discussed in later

sections.

Figures 3E.2-6 a through d show the plots of the 550°F and 350°F stress-strain curves for both the pipe and the plate used in the test. As expected, the weld metal stress-strain curve in every case is higher than the corresponding base metal curve. The Ramberg-Osgood format characterization of these stress-strain curves is given in Section 3E.3.2 where appropriate values of α and n is also provided.

3E.2.2.1.3 J-R Curve Tests

The test temperatures selected for the J-R curve tests were: room temperature, 350°F and 550°F. Both the weld and the base metal were included. Due to the curvature, only the 1T plan compact tension (CT) specimens were obtained from the 16 inch diameter test pipe. Both 1T and 2T plan test specimens were prepared from the test plate. All of the CT specimens were side-grooved to produce plane strain conditions.

Table 3E.2-4 shows some details of the J-R curve tests performed in this test program. The J-R curve in the LC orientation of the pipe base metal and in the LT orientation of the plate base metal represent the material's resistance to crack extension in the circumferential direction. Thus, the test results of these orientations were used in the LBB evaluations. The orientation effects are not present in the weld metal. As an example of the J-R curve obtained in the test program, Figure 3E.2-7 shows the plot of J-R curve obtained from specimen OWLC-A.

3E.2.2.2 Material (J/T) Curve Selection

The normal operating temperatures for most of the carbon steel piping in the reactor coolant pressure boundary in the ABWR generally fall into two categories: 528-550°F and 420°F. The latter temperature corresponds to the operating temperature of the feedwater piping system. The selections of the appropriate material (J/T) curves for these two categories are discussed next.

3E.2.2.2.1 Material J/T curve for 550°F

A review of the test matrix in Table 3E.2-4

shows that 5 tests were conducted at 550°F. Two tests were on the weld metal, two were on the base metal and one was on the heat-affected zone. Figure 3E.2-8 shows the plot of material J_{mod} - T_{mod} values calculated from the J- Δa values obtained from the 550°F tests. The value of flow stress, σ_f , used in the tearing modulus calculation (Equation E.2-1) was 52.0 ksi based on data shown in Table 3E.2-3. To convert the deformation J and $\frac{dJ}{da}$ values obtained from the J-R curve into J_{mod} and T_{mod} , Equations E.2-4 and E.2-6 were used. Only the data from the pipe weld (Specimen ID OWLC-A) and the plate base metal (Specimen ID BMLI-12) are shown in Figure 3E.2-8. A few unreliable data points were obtained in the pipe base metal (Specimen ID OBLC-2) J-R curve test due to a malfunction in the instrumentation. Therefore, the data from this test were not included in the evaluation. The J-R curves from the other two 550°F tests were evaluated as described in the next paragraph. For comparison purposes, Figure 3E.2-8 also shows the SA106 carbon steel J-T data obtained from the J-R curve reported by Gudas [14]. The curve also includes extrapolation to higher J values based on the method recommended in NUREG 1061, Vol. 3 [9].

The J_{mod} - T_{mod} data for the plate weld metal and the plate HAZ were evaluated. A comparison shows that these data fall slightly below those for the plate base metal shown in Figure 3E.2-8. On the other hand, as noted in Subsection 3E.2.2.1.2, the yield strength of the weld metal and the HAZ is considerably higher than that of the base metal. The material stress-strain and J-T curves are the two key inputs in determining the instability load and flaw values by the (J/T) methodology. Calculations performed for representative through-wall flaw sizes showed that the higher yield strength of the weld metal more than compensates for the slightly lower J-R curve and, consequently, the instability load and flaw predictions based on base metal properties are smaller (i.e., conservative). Accordingly, it was concluded that the material (J-T) curve shown in Figure 3E.2-8 is the appropriate one to use in the LBB evaluations for carbon steel piping at 550°F.

3E.2.2.2.2 Material J/T Curve For 420°F

Since the test temperature of 350°F can be considered reasonably close to the 420°F, the test J-R curves for 350°F were used in this case. A review of the test matrix in Table 3E.2-4 shows that three tests were conducted at 350°F. The J_{mod} , T_{mod} data for all three tests were reviewed. The flow stress value used in the tearing modulus calculation was 54 ksi based on Table 3E.2-3. Also reviewed were the data on SA106 carbon steel at 300°F reported by Gudas [14].

Consistent with the trend of the 550°F data, the 350°F weld metal (J-T) data fell below the plate and pipe base metal data. This probably reflects the slightly lower toughness of the SAW weld in the plate. The (J/T) data for the pipe base metal fell between the plate base metal and the plate weld metal. Based on the considerations similar to those presented in the previous section, the pipe base metal J-T data, although they may lie above the weld J-T data, were used for selecting the appropriate (J-T) curve. Accordingly, the curve shown in Figure 3E.2-9 was developed for using the (J-T) methodology in evaluations at 420°F.

~~Subent A~~ see p. 3E.2-5a

3E.2.2.2.2 References

1. Paris, P.C., Tada, H., Zahoor, A., and Ernst, H., "The Theory of Instability of the Tearing Mode of Elastic-Plastic Crack Growth," Elastic-Plastic Fracture, ASTM STP 668, J.D Landes, J.A. Begley, and G.A Clarke, Eds., American Society for Testing Materials, 1979, pp.5-36.
2. "Resolution of the Task A-11 Reactor Vessel Materials Toughness Safety Issue," NUREG-0744, Rev.1 October 1982.
3. Paris, P.C., and Johnson, R.E., "A Method of Application of Elastic-Plastic Fracture Mechanics to Nuclear Vessel Analysis," Elastic-Plastic Fracture, Second Symposium, Volume II-Fracture Resistance Curves and Engineering Application, ASTM STP 803, C.F Shih and J.P. Gudas, Eds., American Society for Testing and Materials, 1983, pp. 11-5-11-40.
4. Rice, J.R., "A Path Independent Integral and the Approximate Analysis of Strain Concentration by Notches and Cracks," J. Appl. Mech., 35, 379-386 (1968).
5. Begley, J.A., and Landes, J.D., "The J Integral as a Fracture Criterion," Fracture Toughness, Proceedings of the 1971 National Symposium on Fracture Mechanics, Part II, ASTM STP 514, American Society for Testing Materials, pp. 1-20 (1972).
6. Hutchinson, J.W., and Paris, P.C., "Stability Analysis of J-Controlled Crack Growth," Elastic-Plastic Fracture, ATSM STP 668, J.D Landes, J.A. Begley, and G.A. Clarke, Eds., American Society for Testing and Materials, 1979, pp. 37-64.
7. Kumar, V., German, M.D., and Shih, C.F., "An Engineering Approach for Elastic-Plastic Fracture Analysis," EPRI Topcal Report NP-1831, Electric Power Research Institute, Palo Alto, CA July 1981.
8. Ernst, H.A., "Material Resistance and Instability Beyond J-Controlled Crack Growth," Elastic-Plastic Fracture: Second Symposium, Volume I--Inelastic Crack Analysis, ASTM STP 803, C.F. Shih and J.P. Gudas, Eds., American Society for Testing and Materials, 1983, pp. 1-191-1-213.
9. Report of the U.S. Nuclear Regulatory Commission Piping Review Committee, NUREG-1061, Vol.3, November 1984.
10. ~~Deleted~~ "Materials and Process Specification - ABWR," General Electric Report No. 22A7014, Rev.B, Sept.1982.
11. ASME Boiler & Pressure Vessel Code, Section III, Division 1, Nuclear Power Plant Components, American Society of Mechanical Engineers, 1980.
12. ASTM Standard E399, "Plane-Strain Fracture Toughness of Metallic Materials."
13. Reynolds, M.B., "Failure Behavior in ASTM A106B Pipes Containing Axial Through-Wall Flaws," General Electric Report No.

continued on p. 3E.2-6

Insert A for Page 3E.2-5

3E2.3 Stainless Steels and Associated Welds

The stainless steels used in the ABWR reactor coolant pressure boundary piping are either Nuclear grade or low carbon Type 304 or 316. These materials and the associated welds are highly ductile and therefore, undergo considerable plastic deformation before failure can occur. Toughness properties of Type 304 and 316 stainless steels have been extensively reported in the open technical literature and are, thus, not discussed in detail in this section. Due to high ductility and toughness, modified limit load methods can be used to determine critical crack lengths and instability loads (see Section 3E.3.3).

GEAP-5620, April 1968.

14. Gudas, J.P., and Anderson, D.R., *"J1-R Curve Characteristics of Piping Material and Welds,"* NUREG/CP-0024, Vol. 3, March 1982.

TABLE 3E.2-1

ELECTRODES AND FILLER METAL REQUIREMENTS
FOR CARBON STEEL WELDS

Base Material	P-No.	Process	Electrode Specification	or	Filler Metal Classification
Carbon Steel to	P-1 to	SMAW	SFA 5.1		E7018
Carbon Steel or	P-1, P-3				
Low Alloy Steel	P-4 or P-5	GTAW PAW	SFA 5.18		E70S-2, E70S-3
		GMAW	SFA 5.18 SFA 5.20		E70S-2, E70S-3, E70S-6 E70T-1
		SAW	SFA 5.17		F72EM12K, F72EL12

TABLE 3E.2-2

SUPPLIER PROVIDED CHEMICAL COMPOSITION AND MECHANICAL PROPERTIES INFORMATION

Material	Product Form	Chemical Composition				Mech. Property			
		C	Mn	P	S	Si	Sy(ksi)	Su(ksi)	Elongation (%)
SA 333 Gr.6 Heat #52339	16 In. Sch.80 Pipe	0.12	1.18	.01	.026	0.27	44.0	67.5	42.0
SA 516 Gr.70 Heat #E18767	1.0 In. Plate	0.18	0.98	0.017	0.0022	0.25	46.5	70.5	31.0

- Note:
- (1) Pipe was normalized at 1650°F. Held for 2 hrs. and air cooled.
 - (2) Plate was normalized at 1700°F for one hour and still air cooled.

TABLE 3E.2-3

STANDARD TENSION TEST DATA AT TEMPERATURE

SPEC. NO.	MATERIAL TEMP	TEST (ksi)	0.2% YS (ksi)	UTS (%)	Elong. %	RA
OW1	PIPE WELD	RT	66.1	81.6	32	77.2
OW2	PIPE WELD	550F	59.0	93.9	24	56.7
ITWL2	PLATE WELD	550F	53.0	91.4	34	51.3
IBL1	PLATE BASE	RT	44.9	73.7	38	51.3
IBL2	PLATE BASE	350F	37.9	64.2	34	68.9
IBL3	PLATE BASE	550F	34.1	69.9	29	59.4
OB1	PIPE BASE	RT	43.6	68.6	41	67.8
OB2	PIPE BASE	350F	42.2	74.9	21	55.4
OB3	PIPE BASE	550F	34.6	78.2	31	55.4

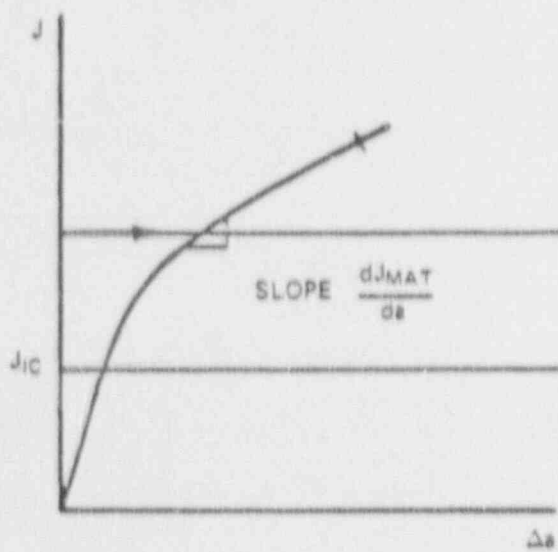
TABLE 3E.2-4

SUMMARY OF CARBON STEEL
J-R CURVE TESTS

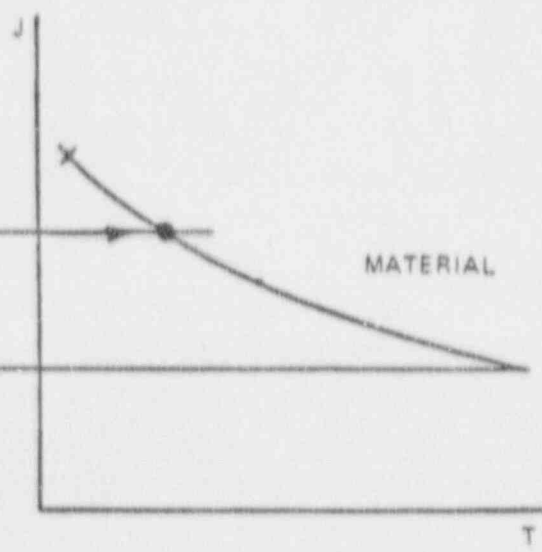
No.	Specimen ID	Size	Description	Temp.
(1)	OWLC-A	1T	Pipe Weld	550°F
(2)	OBCL-1	1T	Pipe Base C-L Orientation	RT
(3)	OBLC2	1T	Pipe Base L-C Orientation	550°F
(4)	OBLC3-B	1T	Pipe Base L-C Orientation	350°F
(5)	BML- ^d	1T	Plate Base Metal, L-T Orientation	RT
(6)	BML4-14	2T	Plate Base Metal, L-T Orientation	RT
(7)	BML2-6	2T	Plate Base Metal, L-T Orientation	350°F
(8)	BML1-12	2T	Plate Base Metal, L-T Orientation	550°F
(9)	WM3-9	2T	Plate Weld Metal	RT
(10)	XWM1-11	2T	Plate Weld Metal	350°F
(11)	WM2-5	2T	Plate Weld Metal	550°F
(12)	HAZ	(Non- standard)	Heat-Affected Zone, Plate Width = 2.793"	RT
(13)	OWLC-7	1T	Pipe Weld	RT

Notes:

1. Pipe base metal, SA333 Gr.6
2. Plate base metal, SA516 Gr.70
3. Pipe weld made by shielded metal arc welding.
4. Plate weld made by submerged arc welding.



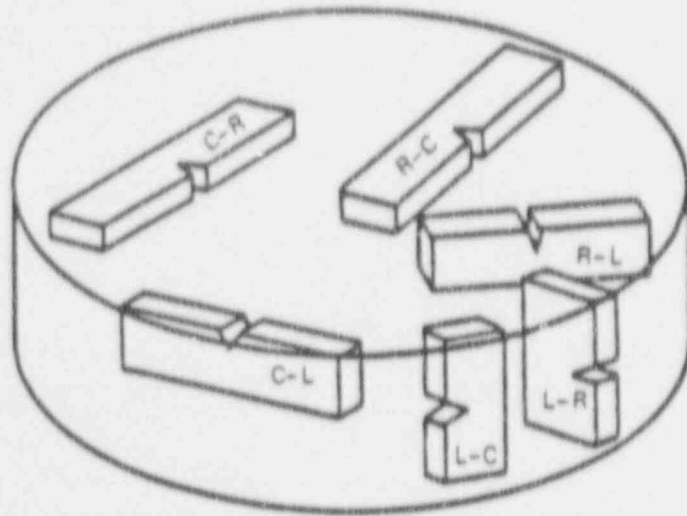
87-632-02



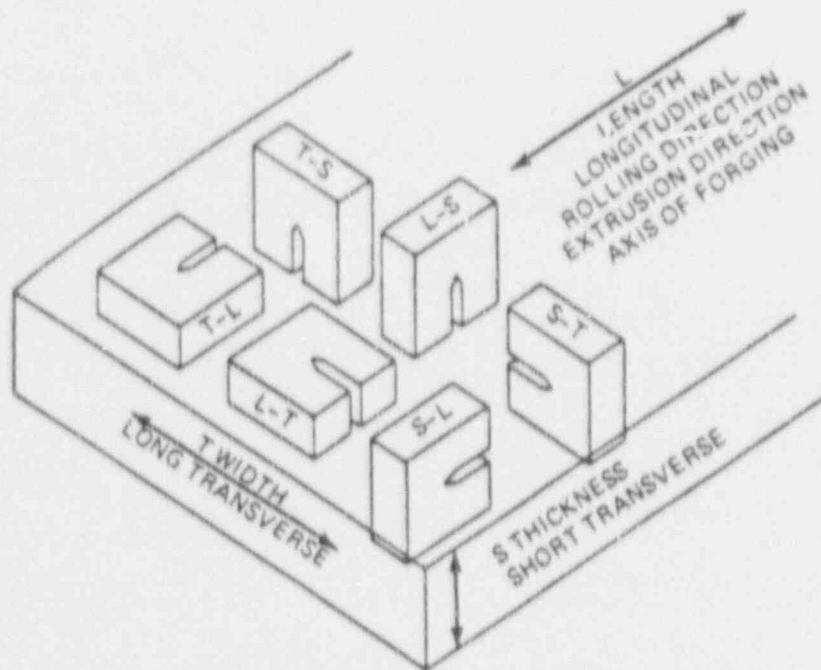
87-592-03

Figure 3E.2-1a SCHEMATIC REPRESENTATION OF MATERIAL J-INTEGRAL R CURVE

Figure 3E.2-1b SCHEMATIC REPRESENTATION OF MATERIAL J-T CURVE



CRACK PLANE ORIENTATION CODE FOR BAR AND HOLLOW CYLINDER



CRACK PLANE ORIENTATION CODE FOR RECTANGULAR SECTIONS

#7-592-04

Figure 3E.2-2 CARBON STEEL TEST SPECIMEN ORIENTATION CODE

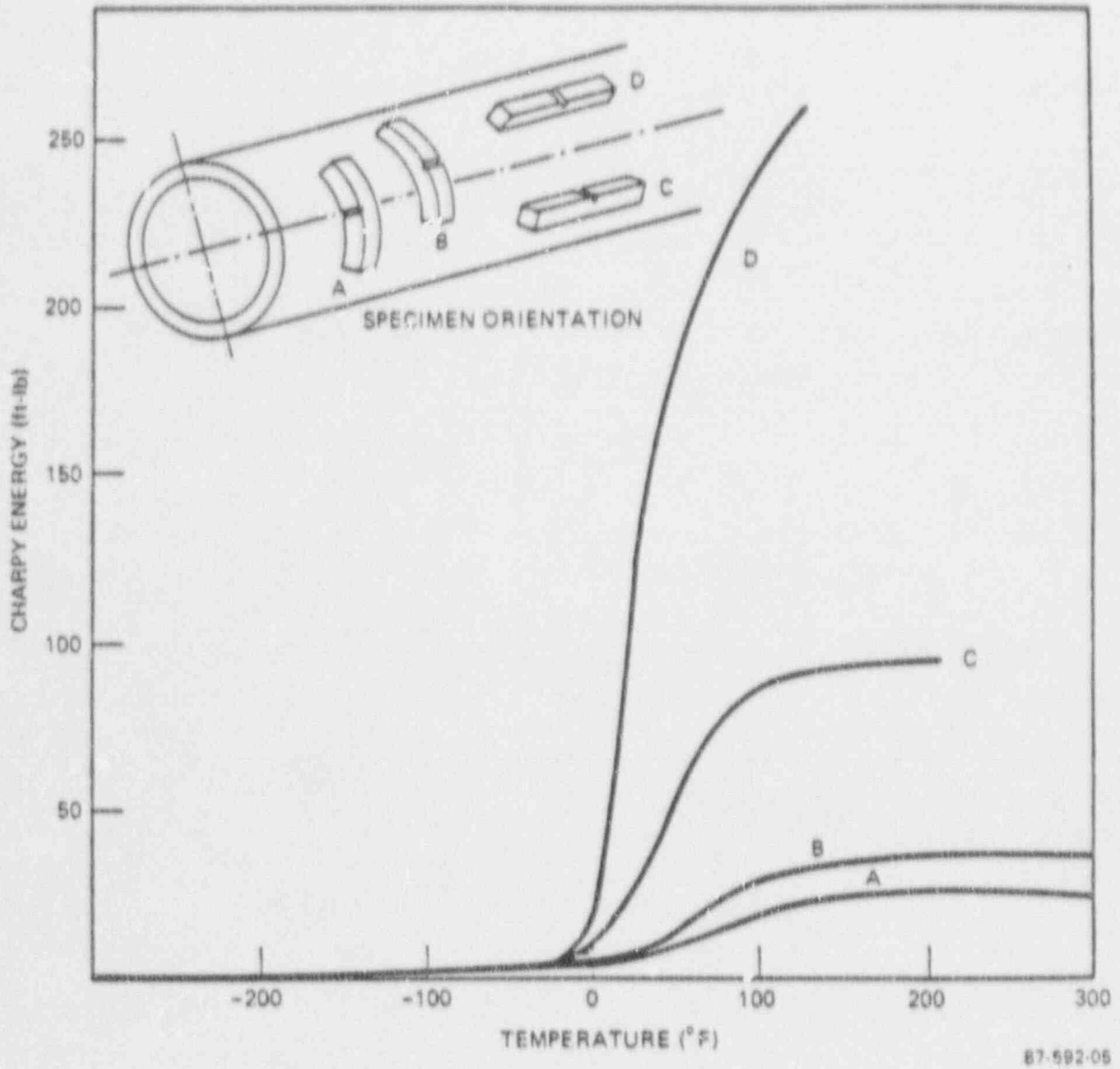
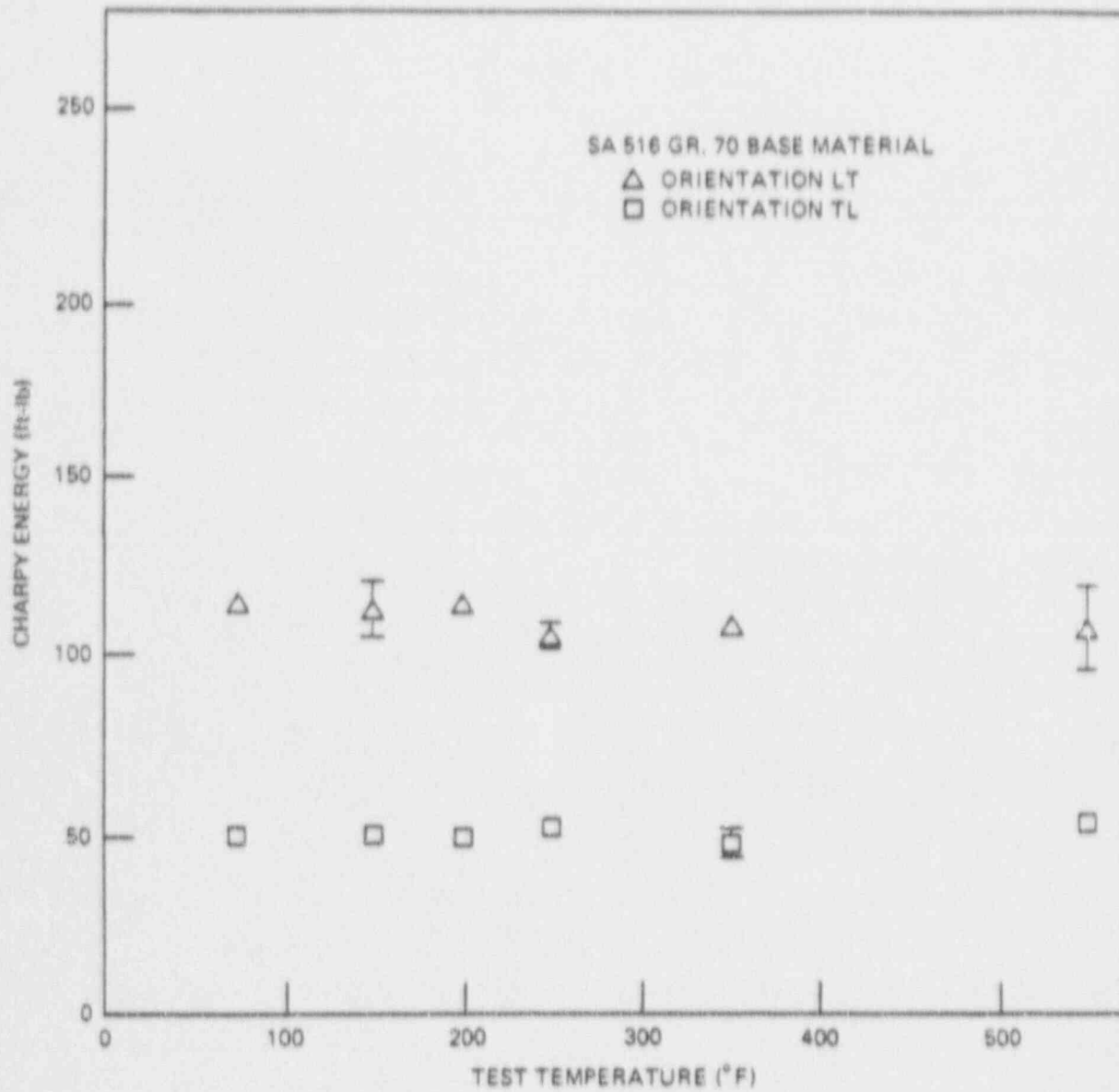
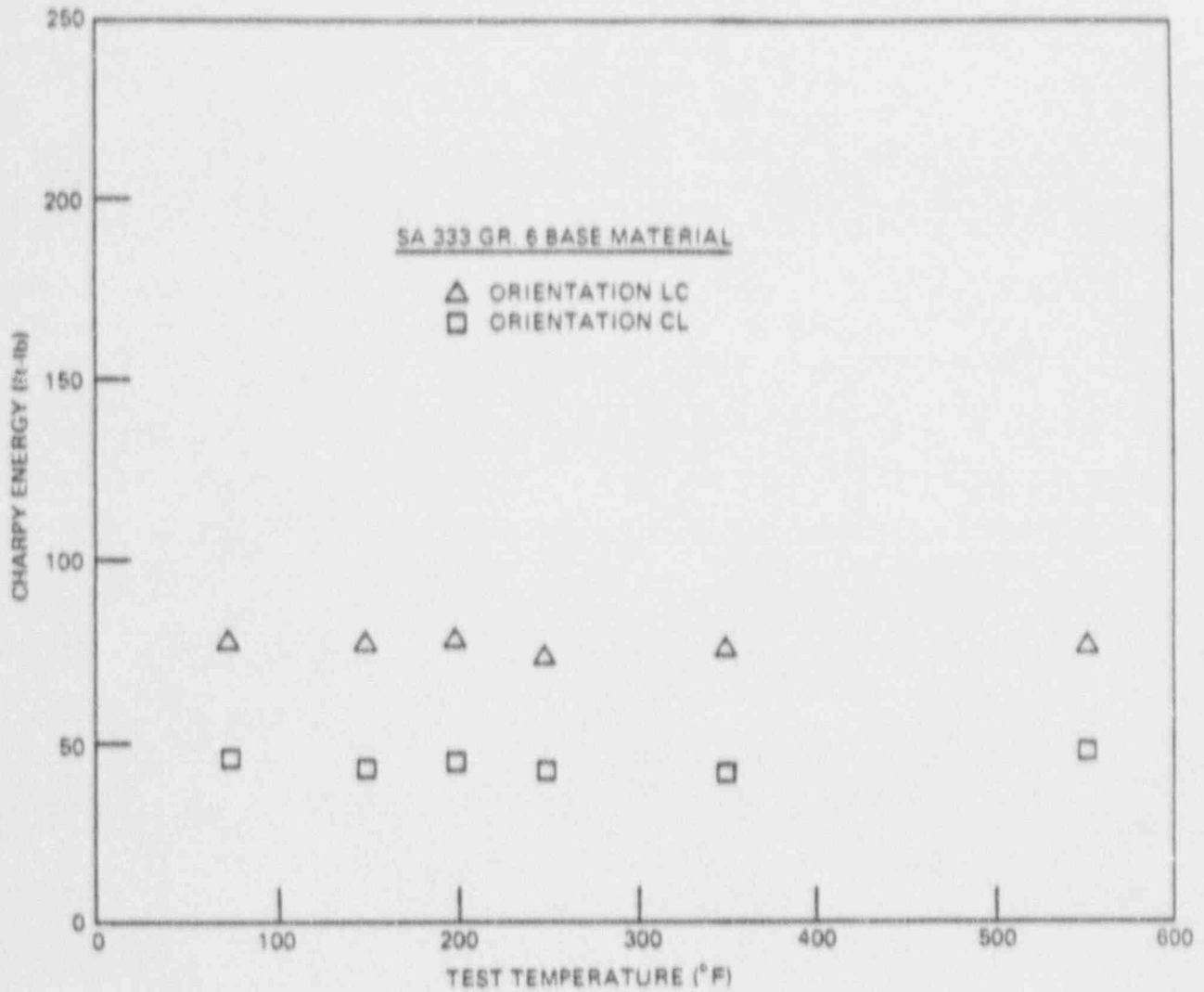


Figure 3E.2-3 TOUGHNESS ANISOTROPY OF ASTM 106 PIPE (6 in. Sch. 80)



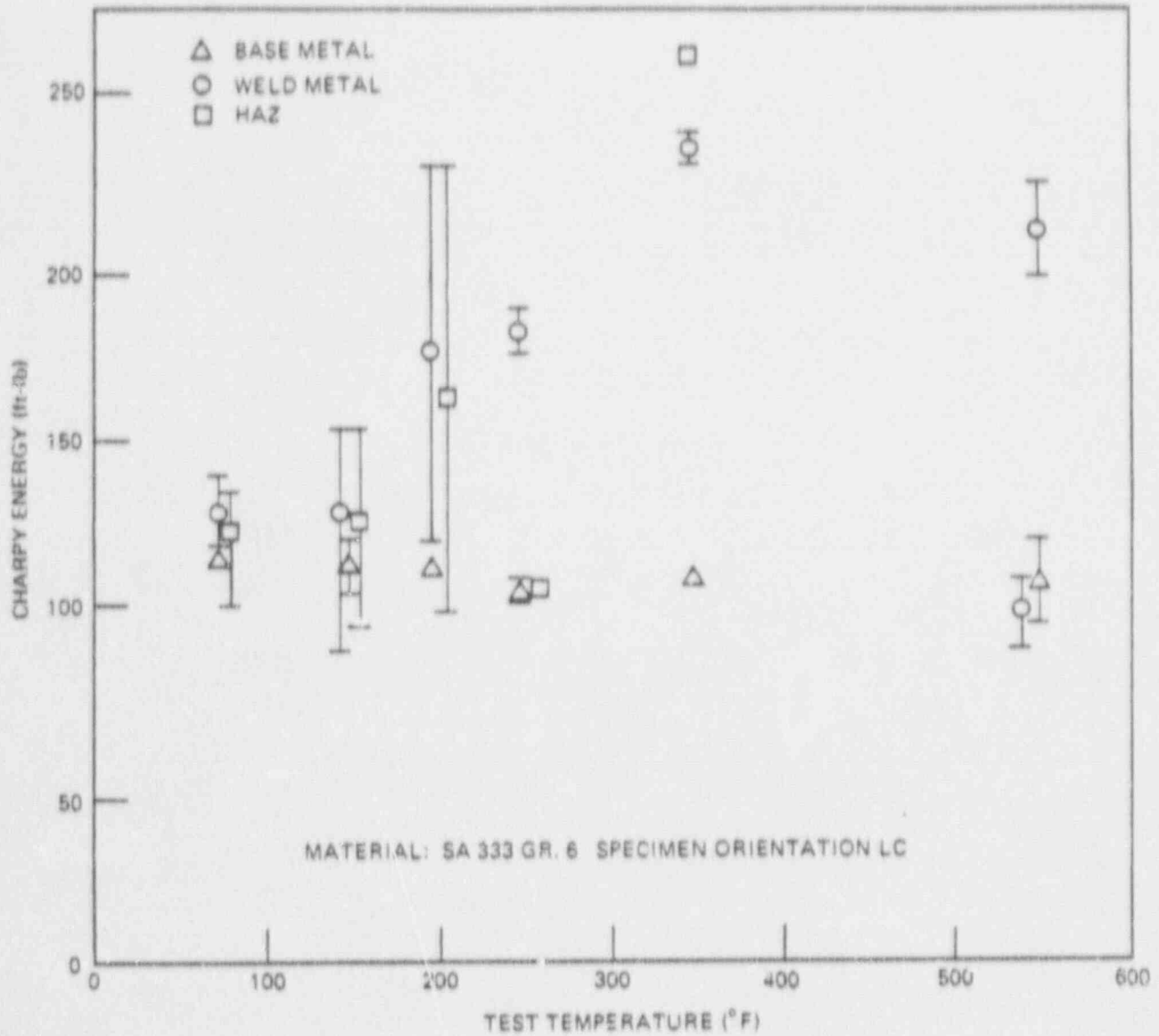
87-592-06

Figure 3E.2-4a CHARPY ENERGIES FOR PIPE TEST MATERIAL AS A FUNCTION OF ORIENTATION AND TEMPERATURE



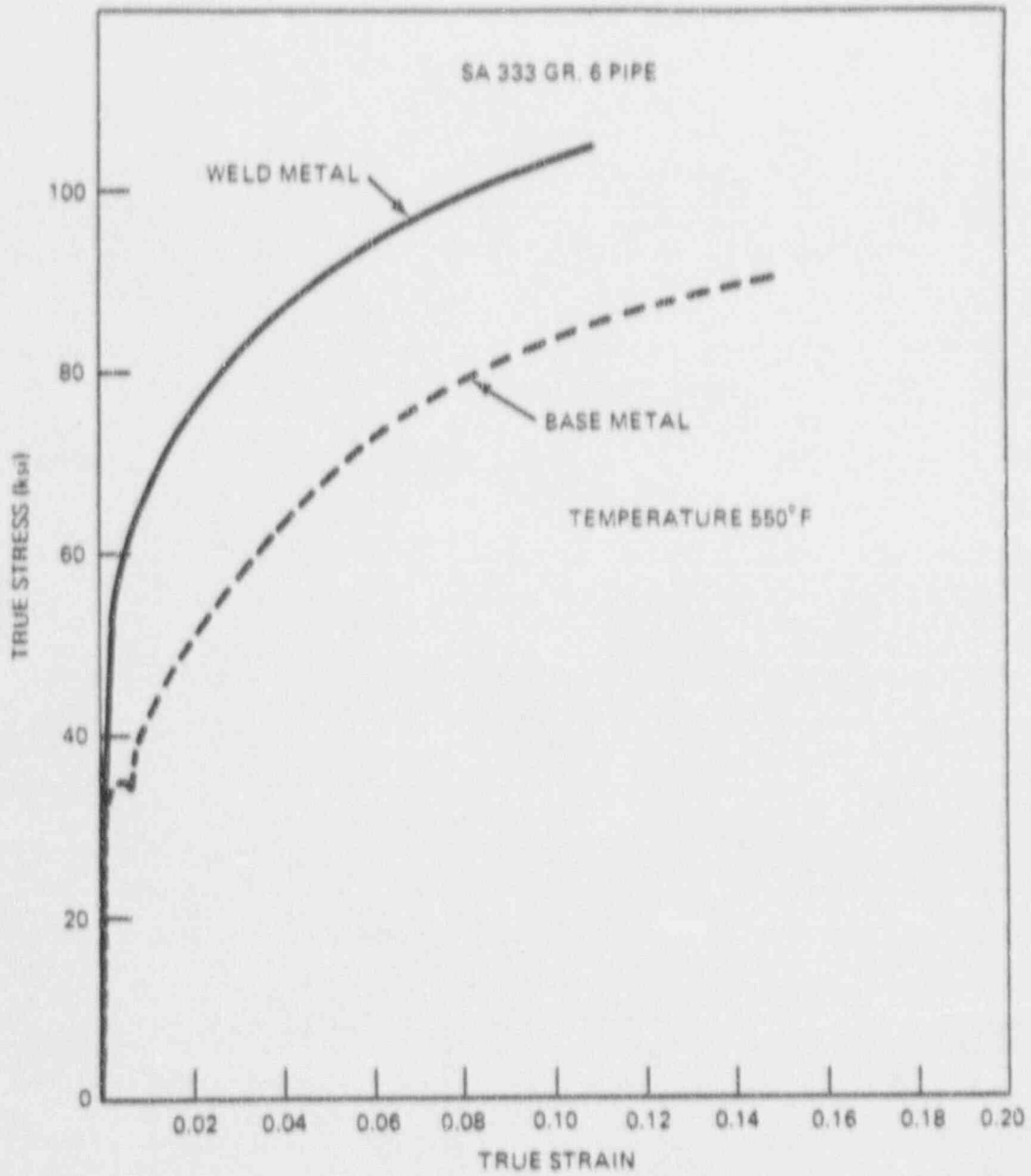
87-592-07

Figure 3E.2-4b CHARPY ENERGIES FOR PLATE TEST MATERIAL AS A FUNCTION OF ORIENTATION AND TEMPERATURE



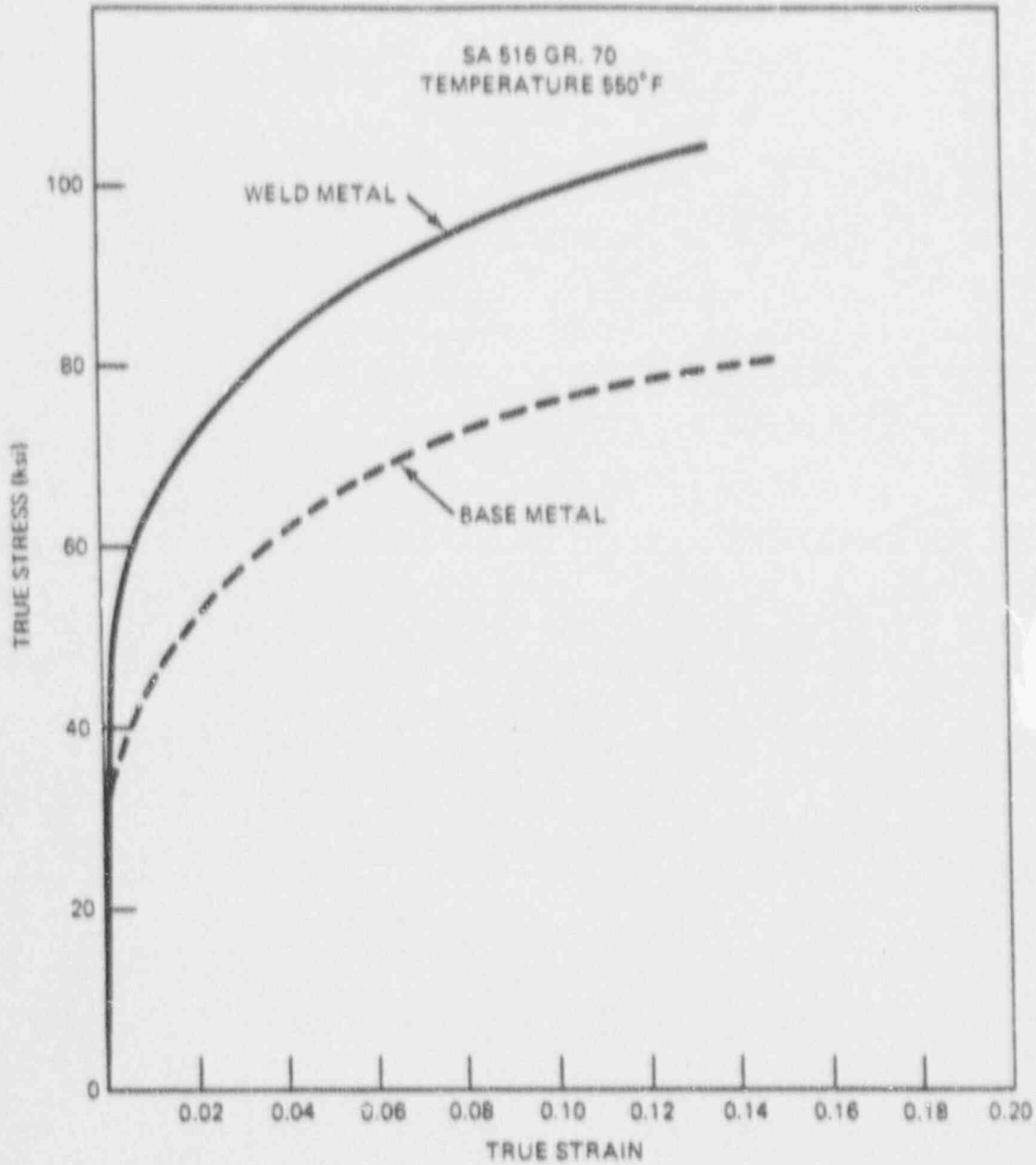
87-592 08

Figure 3E.2-5 COMPARISON OF BASE METAL, WELD AND HAZ CHARPY ENERGIES FOR SA 333 GR. 6



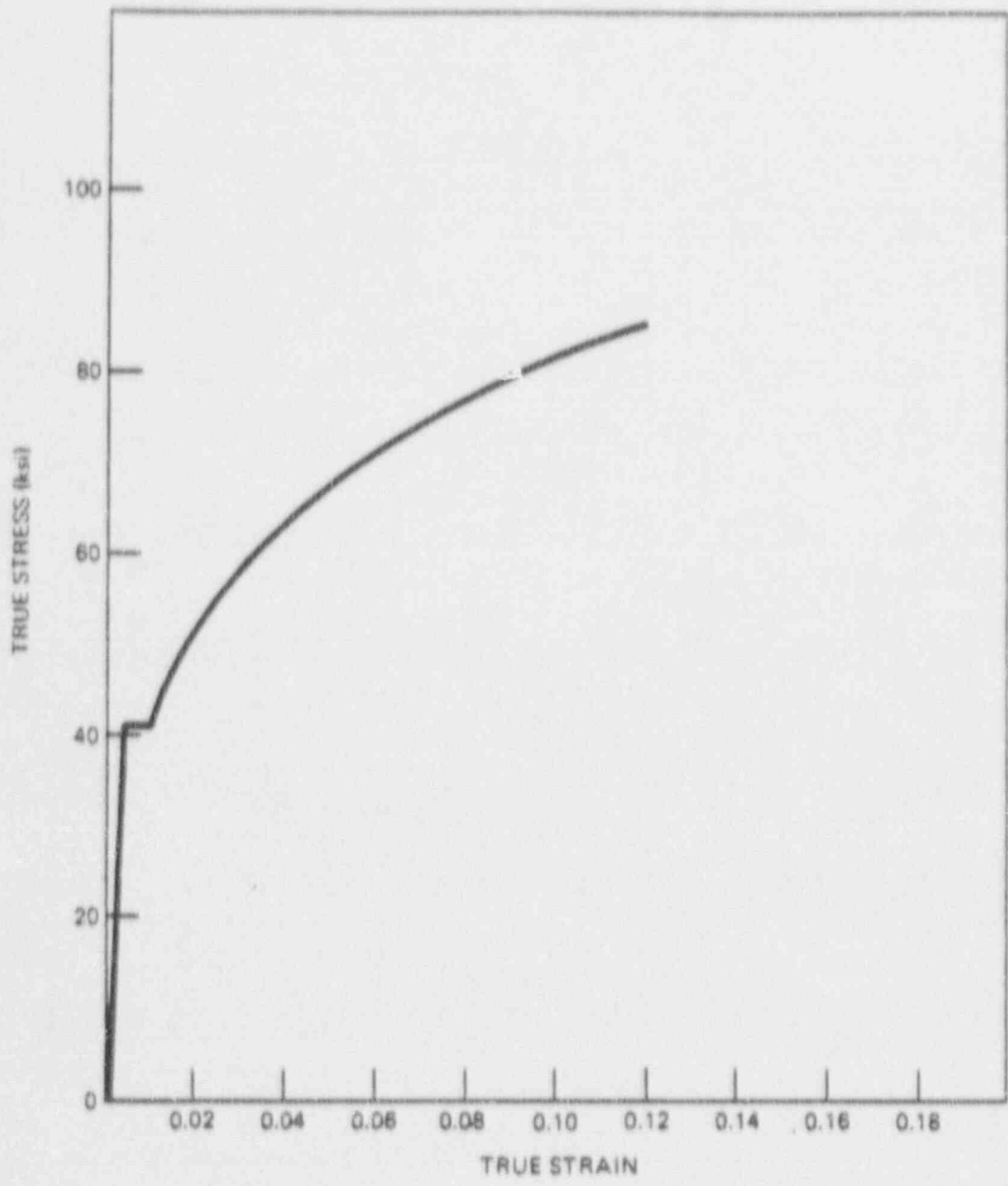
87-592-09

Figure 3E.2-6a PLOT OF 550°F TRUE STRESS-TRUE STRAIN CURVES FOR SA 333 GR. 6 CARBON STEEL



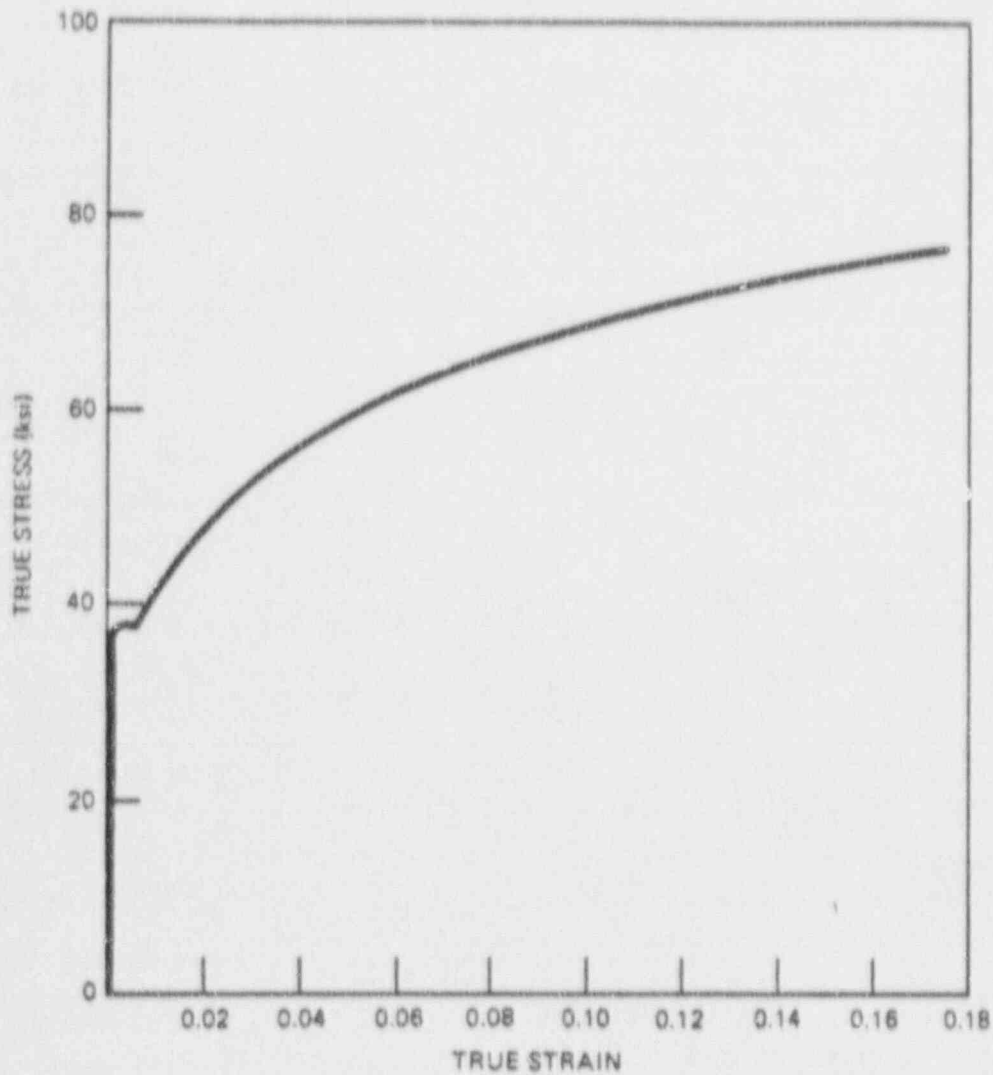
87-582 10

Figure 3E.2-6b PLOT OF 550°F TRUE STRESS-TRUE STRAIN CURVES
FOR SA 516 GR. 70 CARBON STEEL



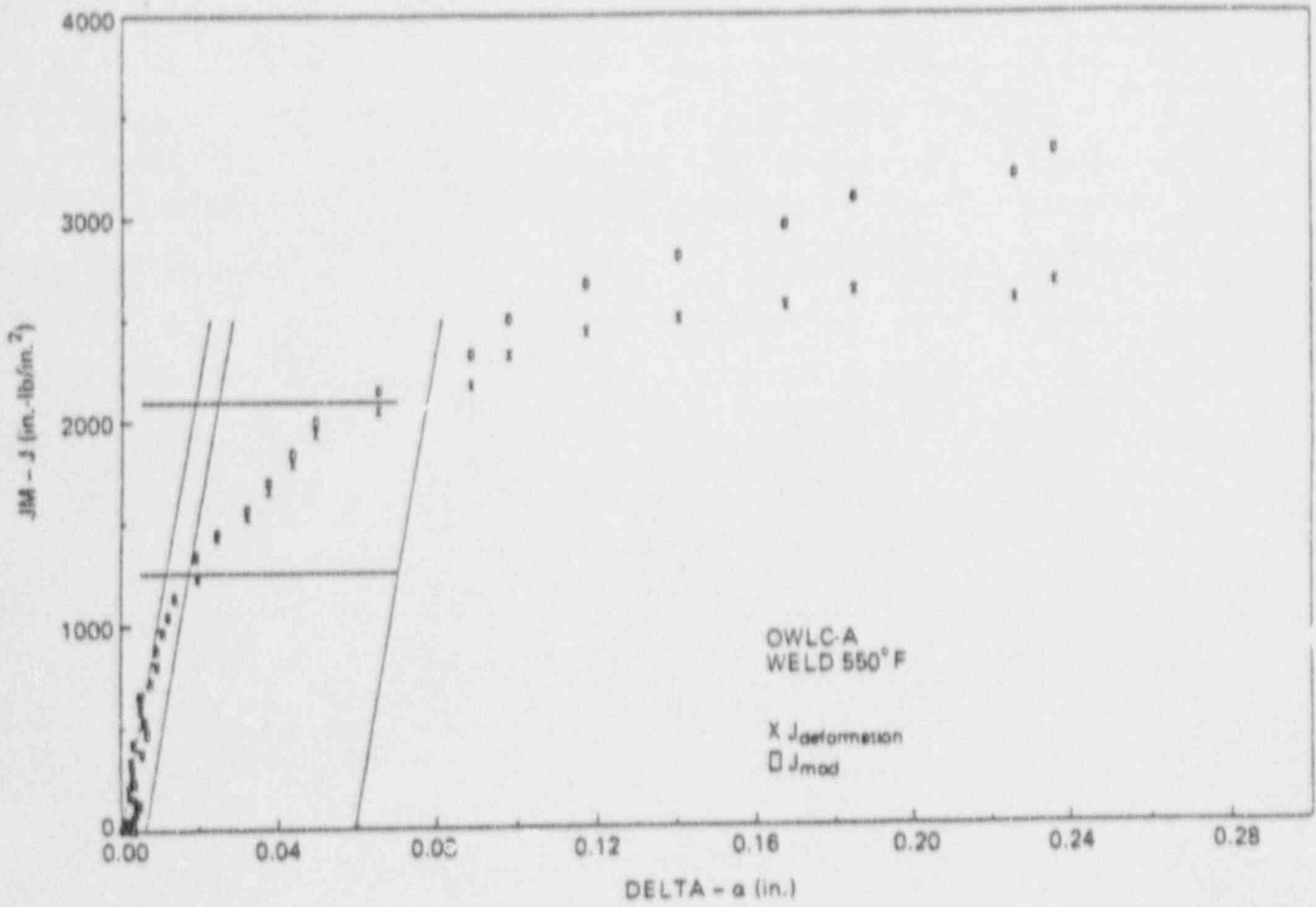
87-592-11

Figure 3E.2-6c PLOT OF 350° F TRUE STRESS-TRUE STRAIN CURVES FOR SA 333 GR. 6 CARBON STEEL



67-592-12

Figure 3E.2--6d PLOT OF 350°F TRUE STRESS-TRUE STRAIN CURVES
FOR SA 516 GR. 70 CARBON STEEL



87-592-13

Figure 3E.2-7 PLOT OF 550°F TEST J-R CURVE FOR PIPE WELD

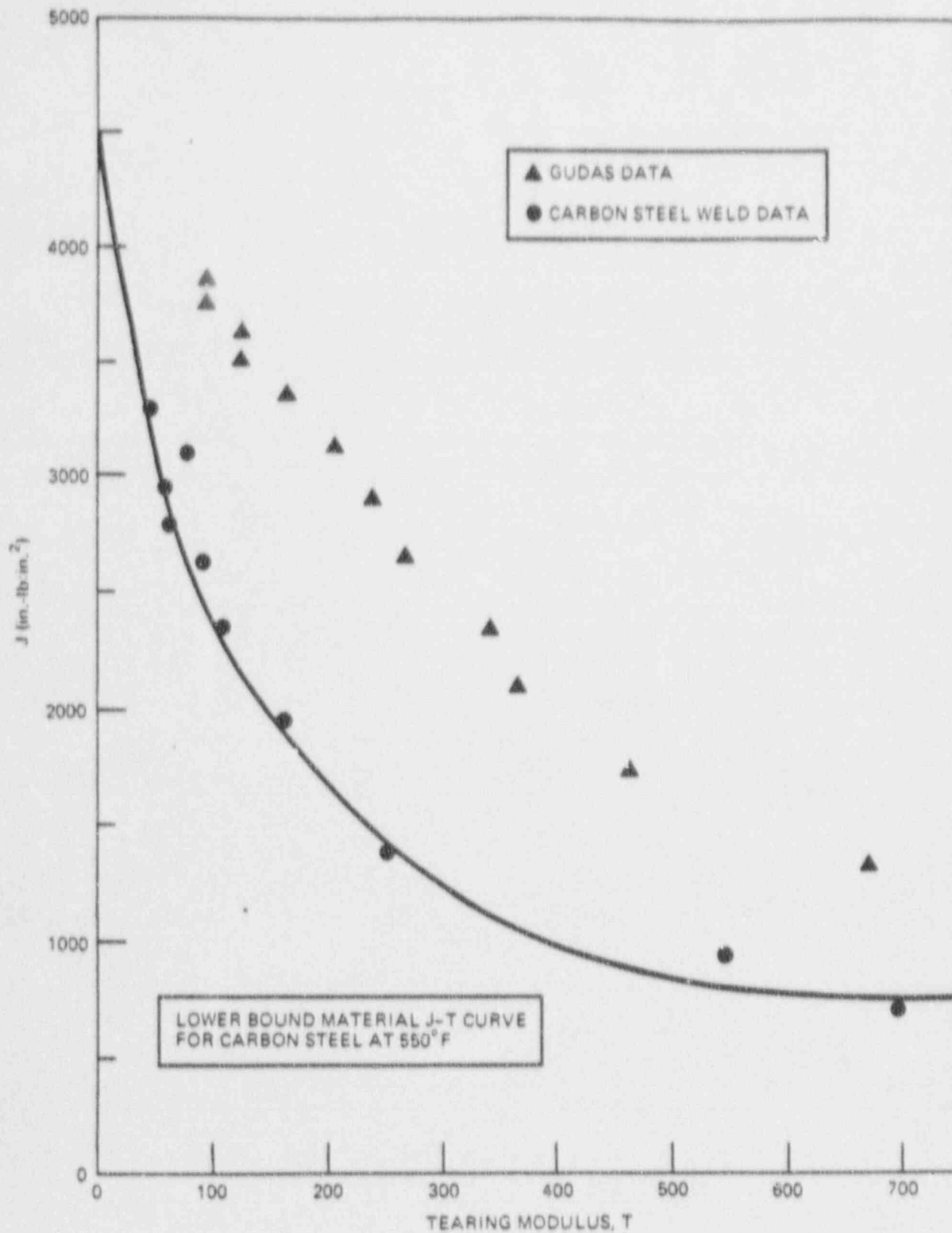
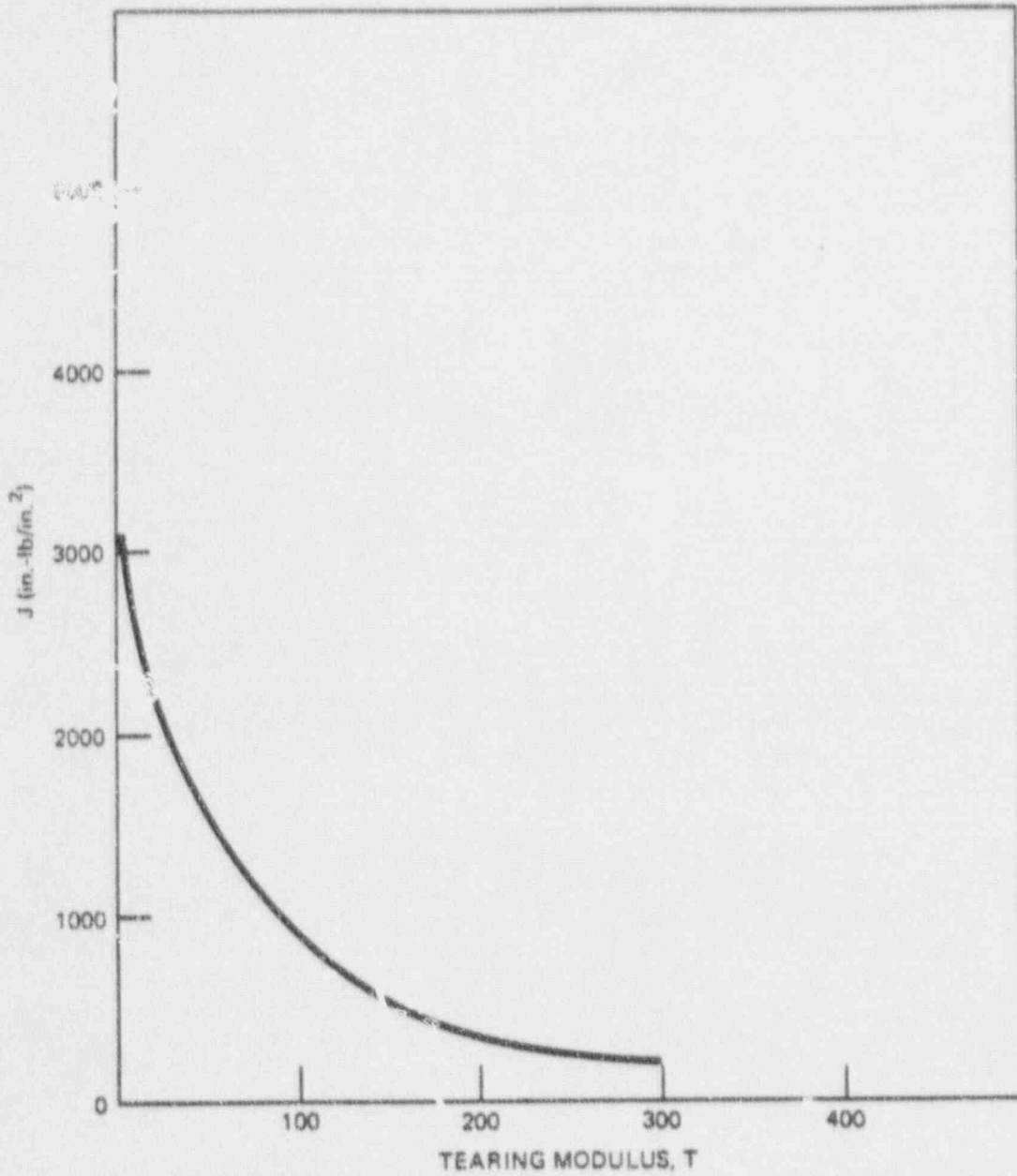


Figure 3E.2-8 PLOT OF 550°F J_{mod} , T_{mod} DATA FROM TEST J-R CURVE



87-5P2-15

Figure 3E.2-9 CARBON STEEL J-T CURVE FOR 420° F

SECTION 3E.3
CONTENTS

<u>Section</u>	<u>Title</u>	<u>Page</u>
3E.3.1	<u>Elastic-Plastic Fracture Mechanics or (J/T) Methodology</u>	3E.3-1
3E.3.1.1	Basic (J/T) Methodology	3E.3-1
3E.3.1.2	J Estimation Scheme Procedure	3E.3-1
3E.3.1.3	Tearing Instability Evaluation Considering Both The Membrane and Bending Stress	3E.3-2
3E.3.2	<u>Application of (J/T) Methodology to Carbon Steel Piping</u>	3E.3-3
3E.3.2.1	Determination of Ramberg-Osgood Parameters For 550° F Evaluation	3E.3-3
3E.3.2.2	Determination of Ramberg-Osgood Parameters For 420° F Evaluation	3E.3-3
3E.3.3	<u>References</u>	3E.3-4

SECTION 3E.3
ILLUSTRATIONS

Figure	Title	Page
3E.3-1	Schematic Illustration of Tearing Stability Evaluation	3E.3-6
3E.3-2	A Schematic Representation of instability Tension and Bending Stresses as a Function of Flaw Length	3E.3-7
3E.3-3	SA 333 Gr. 6 Stress-Strain Data at 550 ^o F in the Ramberg-Osgood Format	3E.3-8
3E.3-4	Carbon Steel Stress-Strain Data at 350 ^o F in the Ramberg-Osgood Format	3E.3-9

3E.3 FRACTURE MECHANICS METHODS

This subsection deals with the fracture mechanics techniques and methods for the determination of critical flaw lengths and instability loads for materials used in ABWR. These techniques and methods comply with Criteria (5) through (11) described in Section 3.6.3, 3E.1.2.

3E.3.1 Elastic-Plastic Fracture Mechanics or (J/T) Methodology

Failure in ductile materials such as highly tough ferritic materials is characterized by considerable plastic deformation and significant amount of stable crack growth. The EPFM approach outlined in this subsection considers these aspects. Two key concepts in this approach are: (1) J-integral [1, 2] which characterizes the intensity of the plastic stress-strain field surrounding the crack tip and (2) the tearing instability theory [3, 4] which examines the stability of ductile crack growth. A key advantage of this approach is that the material fracture toughness characteristic is explicitly factored into the evaluation.

3E.3.1.1 Basic (J/T) Methodology

Figure 3E.3-1 schematically illustrates the J/T methodology for stability evaluation. The material (J/T) curve in Figure 3E.3-1 represents the material's resistance to ductile crack extension. Any value of J falling on the material R-curve is denoted as J_{mat} and is a function solely of the increase in crack length Δa . Also defined in Figure 3E.3-1 is the 'applied' J, which for given stress-strain properties and overall component geometry, is a function of the applied load P and the current crack length, a. Hutchinson and Paris [4] also define the following two nondimensional parameters:

$$T_{applied} = \frac{E}{\sigma_f^2} \cdot \frac{\partial J_{applied}}{\partial a} \quad (3E.3-1)$$

$$T_{mat} = \frac{E}{\sigma_f^2} \cdot \frac{dJ_{mat}}{da}$$

where E is Young's modulus and σ_f is an appropriate flow stress.

Intersection point of the material and applied (J/T) curves denotes the instability point. This is mathematically stated as follows:

$$J_{applied} (a,P) = J_{mat} (a) \quad (3E.3-2)$$

$$T_{applied} < T_{mat} \text{ (stable)} \quad (3E.3-3)$$

$$T_{applied} > T_{mat} \text{ (unstable)}$$

The load at instability is determined from the J versus load plot also shown schematically in Figure 3E.3-1. Thus, the three key curves in the tearing stability evaluation are: $J_{applied}$ versus $T_{applied}$, J_{mat} versus T_{mat} and $J_{applied}$ versus load. The determination of appropriate J_{mat} versus T_{mat} or the material (J/T) curve has been already discussed in subsection 3E.2.1. The $J_{applied}$ - $T_{applied}$ or the (J/T) applied curve can be easily generated through perturbation in the crack length once the $J_{applied}$ versus load information is available for different crack lengths. Therefore, only the methodology for the generation of $J_{applied}$ versus load information is discussed in detail.

3E.3.1.2 J Estimation Scheme Procedure

The $J_{applied}$ or J as a function of load was calculated using the GE/EPRI estimation scheme procedure [5, 6]. The J in this scheme is obtained as sum of the elastic and fully plastic contributions:

$$J = J_e + J_p \quad (3E.3-4)$$

The material true stress-strain curve in the estimation scheme is assumed to be in the Ramberg-Osgood format:

$$\left(\frac{\epsilon}{\epsilon_0} \right) = \left(\frac{\sigma}{\sigma_0} \right) + \alpha \left(\frac{\sigma}{\sigma_0} \right)^n \quad (3E.3-5)$$

where, σ_0 is the material yield stress, $\epsilon_0 = \frac{\sigma_0}{E}$, and α and n are obtained by fitting the preceding equation to the material true stress-strain curve.

The estimation scheme formulas to evaluate

the J-integral for a pipe with a through-wall circumferential flaw subjected to pure tension or pure bending are as follows

Tension

$$J = f_1(a_c, \frac{R}{t}) \frac{P^2}{E} + \alpha \sigma_o \epsilon_o c \left(\frac{a}{b}\right) h_1 \left(\frac{a}{b}, n, \frac{R}{t}\right) \left[\frac{P}{P_o}\right]^{n+1} \quad (3E.3-6)$$

where,

$$f_1 \left(\frac{a}{b}, n, \frac{R}{t}\right) = \frac{a F^2 \left(\frac{a}{b}, n, \frac{R}{t}\right)}{4\pi R^2 t^2}$$

$$P_o = 2 \sigma_o R t \left[\pi - \gamma - 2 \arcsin \left(\frac{1}{2} \sin \gamma \right) \right]$$

Bending

$$J = f_1(a_c, \frac{R}{t}) \frac{M^2}{E} + \alpha \sigma_o \epsilon_o c \left(\frac{a}{b}\right) h_1 \left(\frac{a}{b}, n, \frac{R}{t}\right) \left[\frac{M}{M_o}\right]^{n+1} \quad (3E.3-7)$$

where,

$$f_1 \left(\frac{a}{b}, n, \frac{R}{t}\right) = \frac{\pi a \left(\frac{R}{t}\right)^2 F^2 \left(\frac{a}{b}, n, \frac{R}{t}\right)}{I}$$

$$M_o = M_o \left[\cos \left(\frac{\gamma}{2}\right) - \frac{1}{2} \sin(\gamma) \right]$$

The nondimensional functions F and h are given in Reference 6

While the calculation of J for given α , n, σ_o and load type is reasonably straightforward, one issue that needs to be addressed is the tearing instability evaluation when the loading includes both the membrane and the bending stresses. The estimation scheme is capable of evaluating only one type of stress at a time.

This aspect is addressed next.

3E.3.1.3 Tearing Instability Evaluation
Considering Both the Membrane and Bending Stresses

Based on the estimation scheme formulas and the tearing instability methodology just outlined, the instability bending and tension stresses can be calculated for various through-wall circumferential flaw lengths. Figure 3E.3-2 shows a schematic plot of the instability stresses as a function of flaw length. For the same stress level, the allowable flaw length for the bending is expected to be larger than the tension case.

When the applied stress is a combination of the tension and bending, a linear interaction rule is used to determine the instability stress or conversely the critical flaw length. The application of linear interaction rule is certainly conservative when the instability load is close to the limit load.

The interaction formulas are following: (See Figure 3E.3-2)

Critical Flaw Length (3E.3-8)

$$a_c = \left(\frac{\sigma_t}{\sigma_t + \sigma_b} \right) a_{c,t} + \left(\frac{\sigma_b}{\sigma_t + \sigma_b} \right) a_{c,b}$$

where:

σ_t = applied membrane stress

σ_b = applied bending stress

$a_{c,t}$ = critical flaw length for a tension stress of $(\sigma_t + \sigma_b)$

$a_{c,b}$ = critical flaw length for a bending stress of $(\sigma_t + \sigma_b)$

Instability Bending Stress (3E.3-9a)

$$S_b = \left(1 - \frac{\sigma'_t}{\sigma_t} \right) \sigma'_b$$

where:

- S_b = instability bending stress for flaw length, a , in the presence of membrane stress, σ_t .
- σ_t = applied membrane stress
- σ'_t = instability tension stress for flaw length, a .
- σ'_b = instability bending stress for flaw length, a .

Once the instability bending stress, S_b , in the presence of membrane stress, σ_t , is determined, the instability load margin corresponding to the detectable leak-size crack (as required by LBB criterion in Section 3.6.3) can be calculated as follows:

$$\text{Instability Load Margin} = \frac{\sigma_t + S_b}{\sigma'_t + \sigma'_b} \quad (3E.3-9b)$$

It is assumed in the preceding equation that the uncertainty in the calculated applied stress is essentially associated with the stress due to applied bending loads and that the membrane stress, which is generally due to the pressure loading, is known with greater certainty. This method of calculating the margin against loads is also consistent with the definition of load margin employed in Paragraph IWB-3640 of Section XI [7].

3E.3.2 Application of (J/T) Methodology to Carbon Steel Piping

From Figure 3E.2-3, it is evident that carbon steels exhibit transition temperature behavior marked by three distinct stages: lower shelf, transition and upper shelf. The carbon steels generally exhibit ductile failure mode at or above upper shelf temperatures. This would suggest that a net-section collapse approach may be feasible for the evaluation of postulated flaws in carbon steel piping. Such a suggestion was also made in a review report prepared by the Naval Research Lab [8]. Low temperature (i.e. less than 125°F) pipe tests conducted by GE [9] and by Vassilaros [10] which involved circumferentially cracked pipes subjected to bending and/or pressure loading, also indicate

that a limit load approach is feasible. However, test data at high temperatures specially involving large diameter pipes are currently not available. Therefore, a (J/T) based approach is used in the evaluation.

3E.3.2.1 Determination of Ramberg-Osgood Parameters for 550°F Evaluation

Figure 3E.2-6a shows the true stress-true strain curves for the carbon steels at 550°F. The same data is plotted here in Figure 3E.3-3 in the Ramberg-Osgood format. It is seen that, unlike the stainless steel case, each set for stress-strain data (i.e. data derived from one stress-strain curve) follow approximately a single slope line. Based on the visual observation, a line representing $\alpha = 2$, $n = 5$ in Figure 3E.3-3 was drawn as representing a reasonable upper bound to the data shown.

The third parameter in the Ramberg-Osgood format stress-strain curve is σ_0 , the yield stress. Based on the several internal GE data on carbon steels such as SA 333 Gr.6, and SA 106 Gr.B, a reasonable value of 550°F yield strength was judged as 34600 psi. To summarize, the following values were used in this report for the (J/T) methodology evaluation of carbon steels as 550°F:

- α = 2.0
- n = 5.0
- σ_0 = 34600 psi
- E = 26×10^6 psi

of similar data may be

3E.3.2.2 Determination of Ramberg-Osgood Parameters for 420°F Evaluation

Figure 3E.3-4 shows the Ramberg-Osgood (R-O) format plot of the 350°F true stress-strain data on the carbon steel base metal. Also shown in Figure 3E.3-4 are the CE data a SA 106 Grade B at 400°F. Since the difference between the ASME Code Specified minimum yield strength at 350°F and 420°F is small, the 350°F stress-strain data were considered applicable in the determination of R-O parameters for evaluation at 420°F.

A review of Figure 3E.3-4 indicates that the majority of the data associated with any one test can be approximated by one straight line.

It is seen that some of the data points associated with the yield point behavior fall along the y-axis. However, these data points at low strain level were not considered significant and, therefore, were not included in the R-O fit.

The 350°F yield stress for the base material is given in Table 3E.2-3 as 37.9 ksi. Since the difference between the ASME Code specified minimum yield strengths of pipe and plate carbon steels at 420°F and 350°F is roughly 0.9 ksi, the σ_0 value for use at 420°F are chosen as (37.9 - 0.9) or 37 ksi. In summary, the following values of R-O parameters are used for evaluation of 420°F:

$$\sigma_0 = 37,000 \text{ psi}$$

$$a = 5.0$$

$$n = 4.0$$

Insert A Sec p. 3E.3-4a
3E.3.4 References

1. Rice, J.R., "A Path Independent Integral and the Approximate Analysis of Strain Concentration by Notches and Cracks," J. Appl. Mech., 35, 379-386 (1968).
2. Begley, J.A., and Landes, J.D., "The J Integral as a Fracture Criterion," Fracture Toughness, Proceedings of the 1971 National Symposium on Fracture Mechanics, Part II, ASTM STP 514, American Society for Testing Materials, pp. 1-20 (1972).
3. Paris, P.C., Tada, H., Zahoor, A., and Ernst, H., "The Theory of Instability of the Tearing Mode of Elastic-Plastic Crack Growth," Elastic-Plastic Fracture, ASTM STP 668, J.D. Landes, J.A. Begley, and G.A. Clarke, Eds., American Society for Testing Materials, 1979, pp.5-36.
4. Hutchinson, J.W., and Paris, P.C., "Stability Analysis of J-Controlled Crack Growth," Elastic-Plastic Fracture, ATSM STP

668, J.D. Landes, J.A. Begley, and G.A. Clarke, Eds., American Society for Testing and Materials, 1979, pp. 37-64.

5. Kumar, V., German, M.D., and Shih, C.F., "An Engineering Approach for Elastic-Plastic Fracture Analysis," EPRI Topcal Report NP-1831, Electric Power Research Institute, Palo Alto, CA July 1981.
6. "Advances in Elastic-Plastic Fracture Analysis," EPRI Report No. NP-3607, August 1984.
7. ASME Boiler and Pressure Vessel Code, Section XI, Rules for In-service Inspection of Nuclear Power Plant Components, ASME.
8. Chang, C.I., et al, "Piping Inelastic Fracture Mechanics Analysis," NUREG/CR-1119, June 1980.
9. "Reactor Primary Coolant System Rupture Study Quarterly Progress Report No. 14, July-September, 1968," GEAP-5716, AEC Research and Development Report, December 1968.
10. Vassilaros, M.G., et al, "J-Integral Tearing Instability Analyses for 8-Inch Diameter ASTM A106 Steel Pipe," NUREG/CR-3740, April 1984.
11. Harris, D.O., Lim, EY., and Dedhia, D.D., "Probability of Pipe Fracture in the Primary Coolant Loop of a PWR Plant, Volume 5, Probabilistic Fracture Mechanics Analysis," U.S. Nuclear Regulatory Commission Report NUREG/CR-2189, Volume 5 Washington, DC, 1981.
12. Buchalet, C.B., and Bamford, W.H., "Stress Intensity Factor Solutions for Continuous Surface Flaws in the Reactor Pressure Vessels," Mechanics of Crack Growth, ASTM STP 590. American Society for Testing Materials, 1976, pp. 385-402.
13. Hale, D.A., J.L. Yuen and T.L. Gerber, "Fatigue Crack Growth in Piping and RPV

continued on p. 3E.3-5

Insert A for Page 3E.3-4

3E.3.3 Modified Limit Load Methodology for Austenitic Stainless Steel Piping

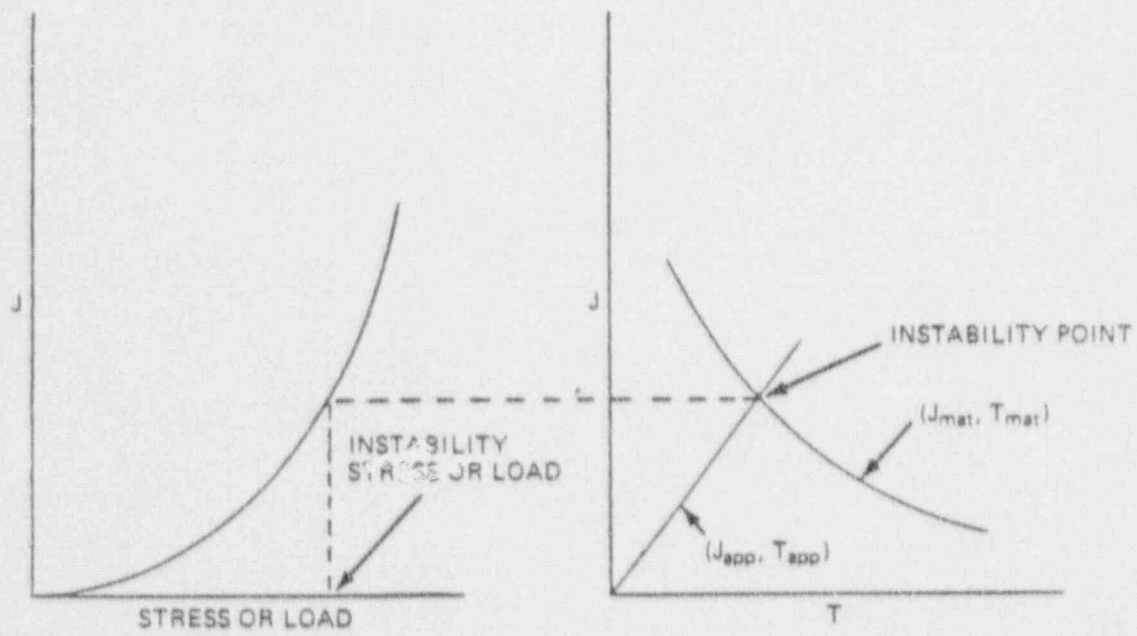
Reference 16 describes a modified limit load methodology that may be used to calculate the critical flaw lengths and instability loads for austenitic stainless steel piping and associated welds. If appropriate, this or an equivalent methodology may be used in lieu of the (J/T) methodology described in 3E.3.1.

ABWR
Standard Plant

23A6100AE
REV. A

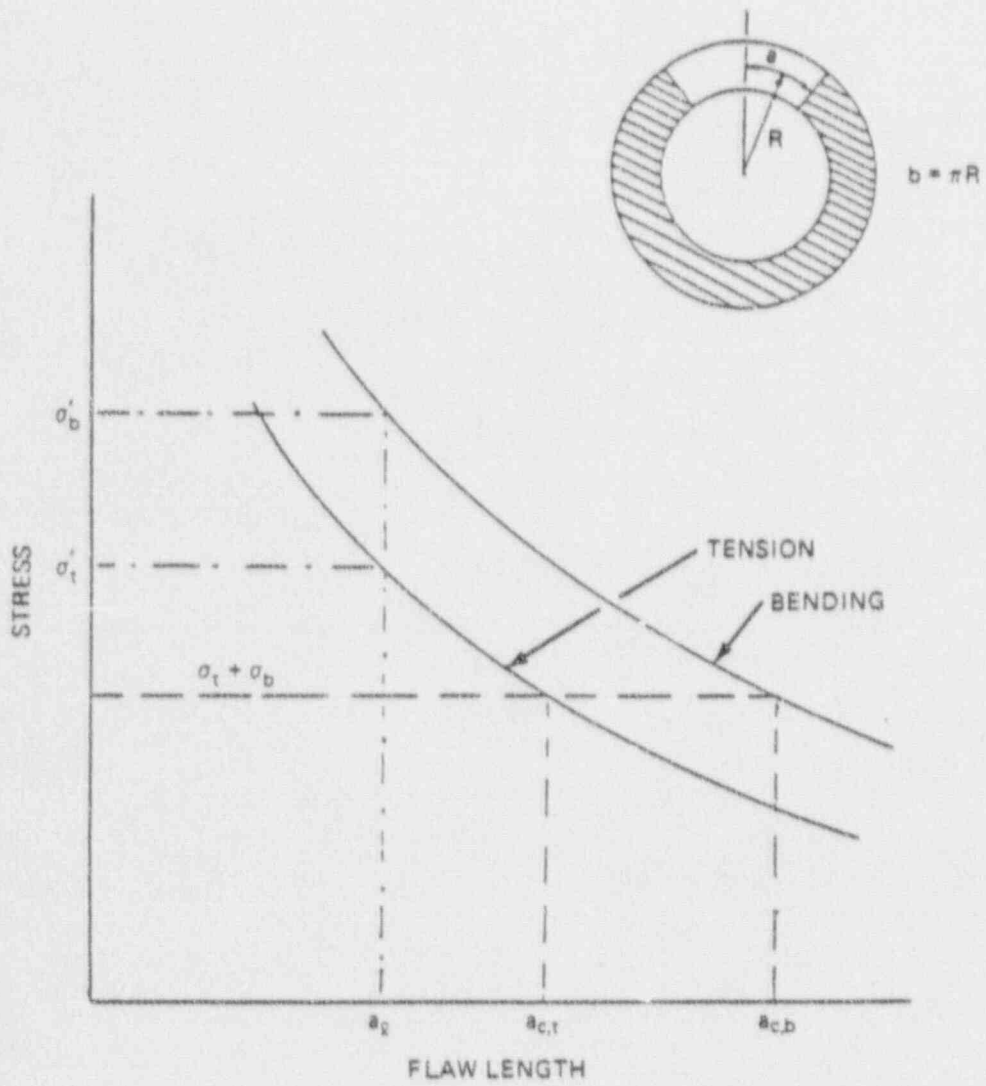
Steels in Simulated BWR Water Environment,
General Electric Report No. GEAP-24098,
January 1978.

14. Hale, D.A., C.W. Jewett and J.N. Kass,
*"Fatigue Crack Growth Behavior of Four
Structural Alloys in High Temperature High
Purity Oxygenated Water,"* Journal of
Engineering Materials and Technology, Vol.
101, July 1979.
15. Hale, D.A., et al, *"Fatigue Crack Growth in
Piping and RPV Steels in Simulated BWR Water
Environment - Update 1981,"* General Electric
Proprietary Report NEDE-24351, July 1981.
16. *Standard Review Plan; Public Comments
Solicited, Federal Register, Volume 52, No.
167, Notices, Pages 32626 to 32633, August
28, 1987.*



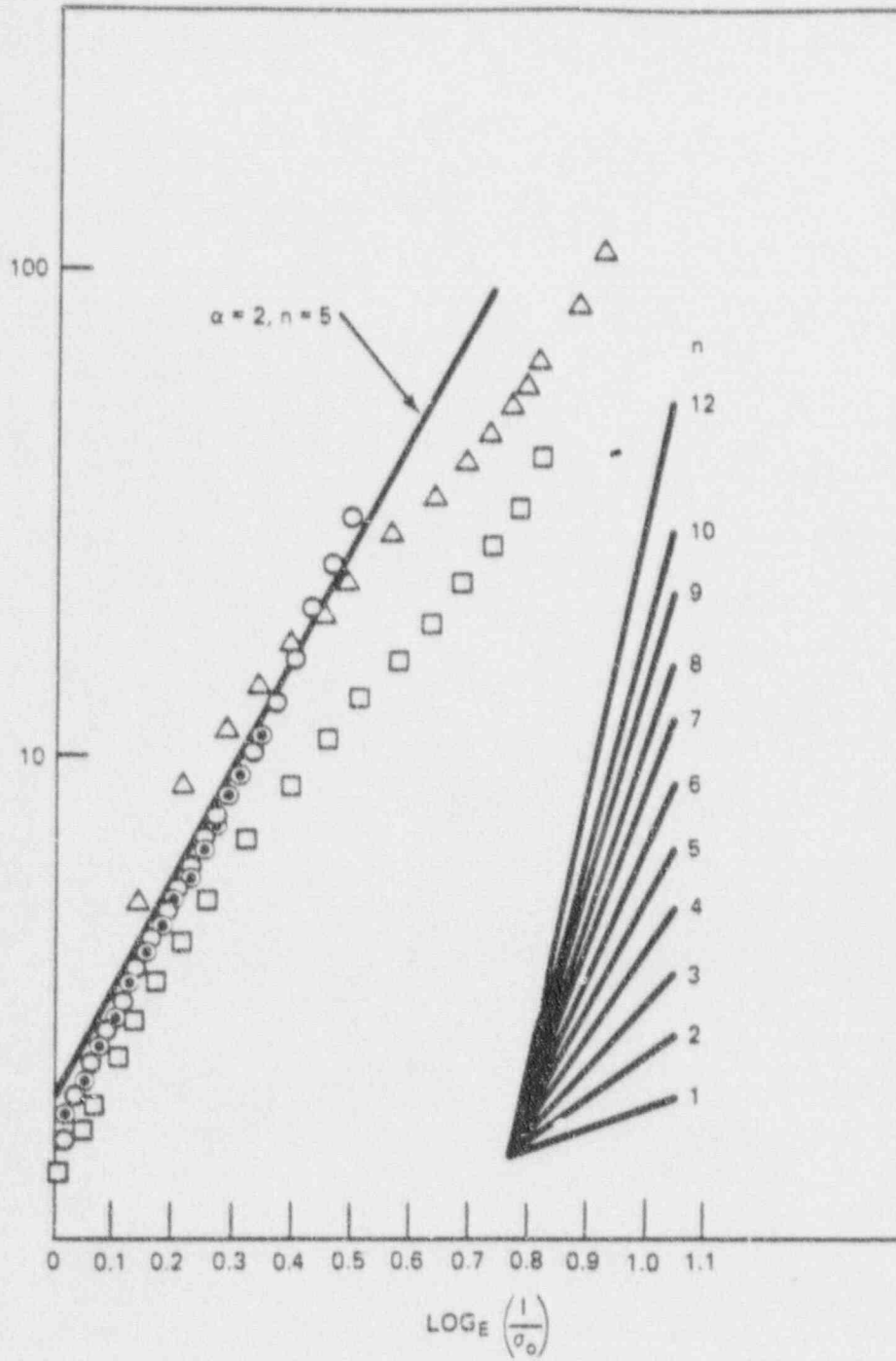
87-592-16

Figure 3E.3-1 SCHEMATIC ILLUSTRATION OF TEARING STABILITY EVALUATION



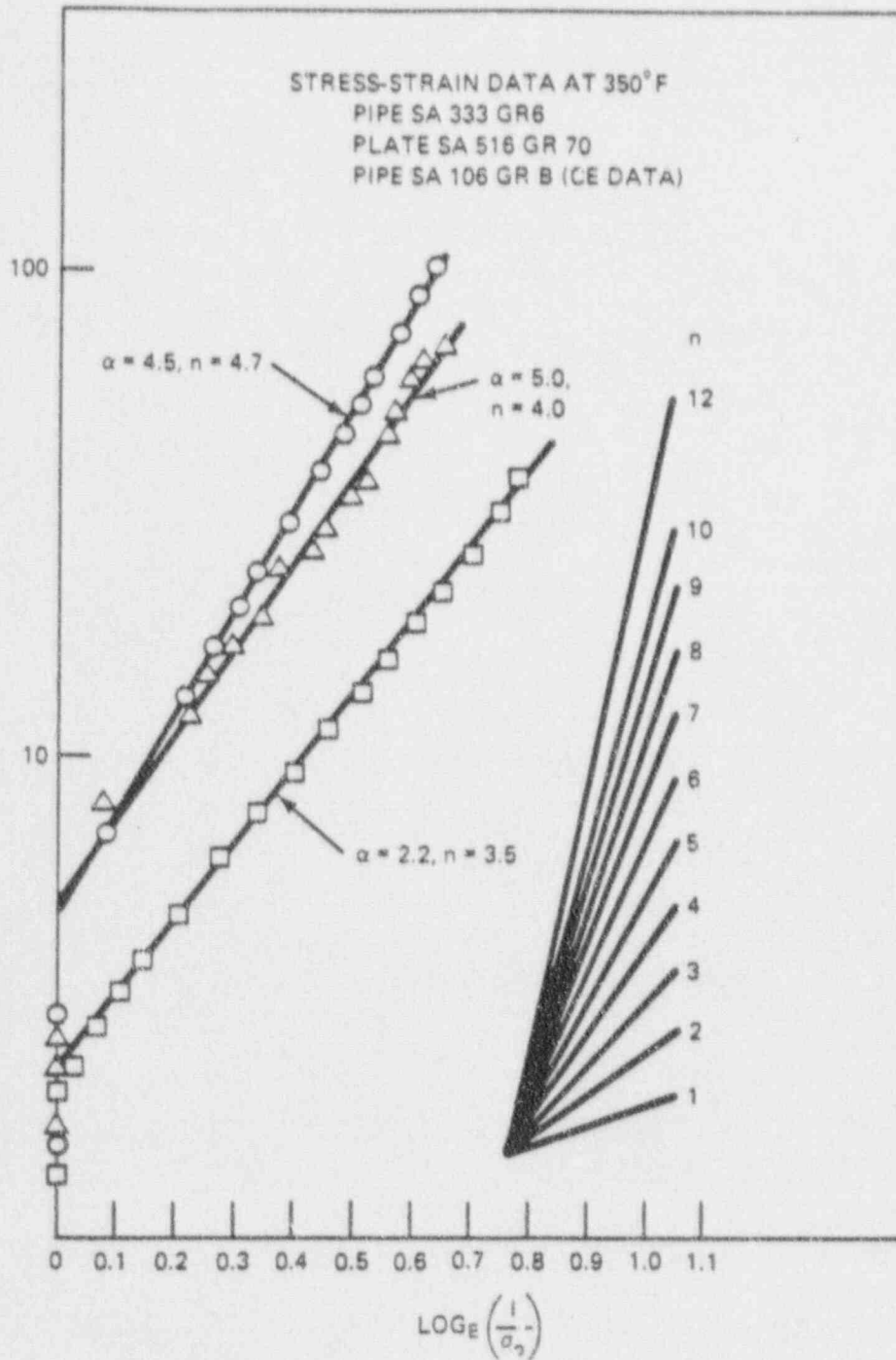
87-592-17

Figure 3E.3-2 A SCHEMATIC REPRESENTATION OF INSTABILITY TENSION AND BENDING STRESSES AS A FUNCTION OF FLAW STRENGTH



87-592-18

Figure 3E.3-3 SA 333 GR. 6 STRESS-STRAIN DATA AT 550°F
IN THE RAMBERG-OSGOOD FORMAT



87-592-19

Figure 3E.3-4 CARBON STEEL STRESS-STRAIN DATA AT 350°F
IN THE RAMBERG-OSGOOD FORMAT

SECTION 3E.4
CONTENTS

<u>Section</u>	<u>Title</u>	<u>Page</u>
3E.4.1	<u>Leak Rate Estimation for Pipes Carrying Water</u>	3E.4-1
3E.4.1.1	Description of Basis for Flow Rate Calculation	3E.4-1
3E.4.1.2	Basis for Crack Opening Area Calculation	3E.4-1
3E.4.1.3	Comparison Verification With Experimental Data	3E.4-2
3E.4.2	<u>Flow Rate Estimation for Saturated Steam</u>	3E.4-2
3E.4.2.1	Evaluation Method	3E.4-2
3E.4.2.2	Selection of Appropriate Friction Factor	3E.4-2
3E.4.2.3	Crack Opening Area Formulation	3E.4-3
3E.4.3	<u>References</u>	3E.4-4

TABLES

<u>Table</u>	<u>Title</u>	<u>Page</u>
3E.4-1	Mass Flow Rate for Several f/D_h Values	3E.4-5

SECTION 3E.4
ILLUSTRATIONS

Figure	Title	Page
3E.4-1	Comparison of PICEP Predictions with Measured Leak Rates	3E.4-6
3E.4-2	Pipe Flow Model	3E.4-7
3E.4-3	Mass Flow Rates for Steam/Water Mixtures	3E.4-8
3E.4-4	Friction Factors for Pipes	3E.4-9

3E.4 LEAK RATE CALCULATION METHODS

Leak rates of high pressure fluids through cracks in pipes are a complex function of crack geometry, crack surface roughness, applied stresses, and inlet fluid thermodynamic state. Analytical predictions of leak rates essentially consist of two separate tasks: calculation of the crack opening area, and the estimation of the fluid flow rate per unit area. The first task requires the fracture mechanics evaluations based on the piping system stress state. The second task involves the fluid mechanics considerations in addition to the crack geometry and its surface roughness information. Each of these tasks are now discussed separately considering the type of fluid state in BWR piping.

3E.4.1 Leak Rate Estimation for Pipes Carrying Water

EPRI-developed computer code PICEP [1] ^{may be} was used in the leak rate calculations. The basis for this code and comparison of its leak rate predictions with the experimental data is described in References 2 and 3. This code ~~was~~ ^{has been} also recently used in the successful application of LBB to primary piping system of a PWR. The basis for flow rate and crack opening area calculations in PICEP is briefly described first. A comparison with experimental data is shown next.

3E.4.1.1 Description of Basis for Flow Rate Calculation

The thermodynamic model implemented in PICEP computer program assumes the leakage flow through pipe cracks to be isenthalpic and homogeneous, but it accounts for non-equilibrium "flashing" transfer process between the liquid and vapor phases.

Fluid friction due to surface roughness of the walls and curved flow paths has been incorporated in the model. Flows through both parallel and convergent cracks can be treated. Due to the complicated geometry within the flow path, the model uses some approximations and empirical factors which were confirmed by comparison against test data.

Other methods (e.g., Reference 4) may be used for leak rate estimation at the discretion of the applicant.

For given stagnation conditions and crack geometries, the leak rate and exit pressure are calculated using an iterative search for the exit pressure starting from the saturation pressure corresponding to the upstream temperature and allowing for friction, gravitational, acceleration and area change pressure drops. The inertial flow calculation is performed when the critical pressure is lowered to the back pressure without finding a solution for the critical mass flux.

A conservative methodology was developed to handle the flow of two-phase mixture or superheated steam through a crack. To make the model continuous, a correction factor was applied to adjust the mass flow rate of a saturated mixture to be equal to that of a slightly subcooled liquid. Similarly, a correction factor was developed to ensure continuity as the steam became superheated. The superheated model was developed by applying thermodynamic principles to an isentropic expansion of the single phase steam.

The code can calculate flow rates through fatigue or IGSCC cracks and has been verified against data from both types. The crack surface roughness and the number of bends account for the difference in geometry of the two types of cracks. The guideline for predicting leak rates through IGSCCs when using this model was based on obtaining the number of turns that give the best agreement for Battelle Phase II test data of Collier et al. [4].⁵ For fatigue cracks, it is assumed that the crack path has no bends.

3E.4.1.2 Basis for Crack Opening Area Calculation

The crack opening area in PICEP code is calculated using the estimation scheme formulas. The plastic contribution to the displacement is computed by summing the contributions of bending and tension alone, a procedure that underestimates the displacement from combined tension and bending. However, the plastic contribution is expected to be insignificant because the applied stresses at normal operation are generally such that they do not produce significant plasticity at the cracked location.

3E.4.1.3 Comparison Verification with Experimental Data

Figure 3E.4-1 from Reference 3 shows a comparison PICEP prediction with measured leak rate data. It is seen that PICEP predictions are virtually always conservative (i.e., the leak flow rate is underpredicted).

3E.4.2 Flow Rate Estimation for Saturated Steam

3E.4.2.1 Evaluation Method

The calculations for this case were based on the maximum two-phase flow model developed by Moody [Reference 5]. This model predicts the flow rate of steam-water mixtures in vessel blowdown from pipes (see Figure 3E.4-2). A key parameter that characterized the flow passage in the Moody analysis is fL/D_h , where, f is the coefficient of friction, L , the length of the flow passage and D_h , the hydraulic diameter. The hydraulic diameter for the case of flow through a crack is 2δ where δ is the crack opening displacement and the length of the flow passage is t , the thickness of the pipe. Thus, the parameter fL/D_h in the Moody analysis was interpreted as $ft/2\delta$ for the purpose of this evaluation.

Figure 3E.4-3 shows the predicted mass flow rates by Moody for fL/D_h of 0 and 1. Similar plots are given in Reference 5 for additional fL/D_h values of 2 through 100. Since the steam in the ABWR main steam lines would be essentially saturated, the mass flow rate corresponding to the upper saturation envelope line is the appropriate one to use. Table 3E.4-1 shows the mass flow rates for a range of fL/D_h values for a stagnation pressure of 1000 psi which is roughly equal to the pressure in an ABWR piping system carrying steam.

A major uncertainty in calculating the leakage rate is the value of f . This is discussed next.

3E.4.2.2 Selection of Appropriate Friction Factor

Typical relationships between Reynolds' Number and relative roughness ϵ/D_h , the ratio of

effective surface protrusion height to hydraulic diameter, were relied upon in this case. Figure 3E.4-4, from Reference 6, graphically shows such a relationship for pipes. The ϵ/D_h ratio for pipes generally ranges from 0 to 0.50. However, for a fatigue crack consisting of rough fracture surfaces represented by a few mils, the roughness height ϵ at some location may be almost as much as δ . In such cases, ϵ/D_h would seem to approach 1/2. There are no data or any analytical model for such cases, but a crude estimate based on the extrapolation of the results in Figure 3E.4-4 would indicate that f may be of the order of 0.1 to 0.2. For this evaluation an average value of 0.15 was used with the modification as discussed next.

For blowdown of saturated vapor, with no liquid present, Moody states that the friction factor should be modified according to

(3E.4-1)

$$f_g = f_{GSP} \left[\frac{\nu_l}{\nu_g} \right]^{1/3}$$

where

f_g = modified friction factor

f_{GSP} = factor for single phase

ν_l = liquid/vapor specific volume ratio evaluated at an average static pressure in the flow path

This correction is necessary because the absence of a liquid film on the walls of the flow channel at high quality makes the two-phase flow model invalid as it stands. The average static pressure in the flow path is going to be something in excess of 500 psia if the initial pressure is 1000 psia; this depends on the amount of flow choking and can be determined from Reference 6. However, a fair estimate of $(\nu_l/\nu_g)^{1/3}$ is ≈ 0.3 , so the friction factor for saturated steam blowdown may be taken as 0.3 of that for mixed flow.

Based on this discussion, a coefficient of friction of $0.15 \times 0.3 = 0.045$ was used in the flow rate estimation. Currently experimental data are unavailable to validate this assumed value of coefficient of friction.

3E.4.2.3 Crack Opening Area Formulation

The crack opening areas were calculated using LEFM procedures with the customary plastic zone correction. The loadings included in the crack opening area calculations were: pressure, weight and thermal expansion.

The mathematical expressions given by Paris and Tada [7] are used in this case. The crack opening areas for pressure (A_p) and bending stresses (A_b) were separately calculated and then added together to obtain the total area, A_c .

For simplicity, the calculated membrane stresses from weight and thermal expansion loads were combined with the axial membrane stress, σ_p , due to the pressure.

The formulas are summarized below:

$$A_p = \frac{\sigma_p}{E} (2\pi R t) G_p(\lambda) \quad (3E.4-2)$$

where,

σ_p = axial membrane stress due to pressure, weight and thermal expansion loads.

E = Young's modulus

R = pipe radius

t = pipe thickness

λ = shell parameter = a/\sqrt{Rt}

a = half crack length

(3E.4-3)

$$G_p(\lambda) = \lambda^2 + 0.16 \lambda^4 \quad (0 \leq \lambda \leq 1)$$

$$= 0.02 + 0.81 \lambda^2 + 0.30 \lambda^3$$

$$+ 0.03 \lambda^4 \quad (1 \leq \lambda \leq 5)$$

$$A_b = \frac{\sigma_b}{E} \cdot \pi \cdot R^2 \cdot \frac{(3 + \cos \theta)}{4} I_t^{(\theta)} \quad (3E.4-4)$$

where,

σ_b = bending stress due to weight and thermal expansion loads

θ is half crack angle

(3E.4-5)

$$I_t(\theta) = 2\theta^2 \left[1 + \left(\frac{\theta}{\pi}\right)^3/2 \right. \\ \left. \left\{ 8.6 - 13.3 \left(\frac{\theta}{\pi}\right) + 24 \left(\frac{\theta}{\pi}\right)^2 \right\} \right. \\ \left. + \left(\frac{\theta}{\pi}\right)^3 \left\{ 22.5 - 7.9 \left(\frac{\theta}{\pi}\right) + 205.7 \left(\frac{\theta}{\pi}\right)^2 \right. \right. \\ \left. \left. - 247.5 \left(\frac{\theta}{\pi}\right)^3 + 242 \left(\frac{\theta}{\pi}\right)^4 \right\} \right]$$

($0 < \theta < 100^\circ$)

The plastic zone correction was incorporated by replacing a and θ in these formulas by a_e and θ_e which are given by

$$\theta_{eff} = \theta + \frac{K_{total}^2}{2\pi R \sigma_Y} \quad (3E.4-6)$$

$$a_e = \theta_e \cdot R$$

The yield stress, σ_y , was conservatively assumed as the average of the code specified yield and ultimate strength. The stress intensity factor, K_{total} , includes contribution due to both the membrane and bending stress and is determined as follows:

$$K_{total} = K_m + K_b \quad (3E.4-7)$$

where,

$$K_m = \sigma_p \sqrt{a} \cdot F_p(\lambda)$$

$$F_p(\lambda) = (1 + 0.3225 \lambda^2)^{\frac{1}{2}}$$

$$= 0.9 + 0.25 \lambda \quad \begin{matrix} (0 \leq \lambda \leq 1) \\ (1 \leq \lambda \leq 5) \end{matrix}$$

$$K_b = \sigma_b \cdot \sqrt{\pi a} \cdot F_b(\theta)$$

$$F_b(\theta) = 1 + 6.8 \left(\frac{\theta}{\pi}\right)^{3/2}$$

$$- 13.6 \left(\frac{\theta}{\pi}\right)^{5/2} + 20 \left(\frac{\theta}{\pi}\right)^{7/2}$$

$$(0 \leq \theta \leq 100^\circ)$$

The steam mass flow rate, M, shown in Table 3E.4-1 is a function of parameter, ft/2δ. Once the mass flow rate is determined corresponding to the calculated value of this parameter, the leak rate in gpm can then be calculated.

3E.4.3 References

1. Norris, D., B. Chexal, T. Griesbach. 1987. PICEP: Pipe Crack Evaluation Program, NP-3596-SR, Special Report, Rev. 1, Electric Power Research Institute, Palo Alto, CA.

2. Chexal, B. & J. Horowitz. A Critical Flow Model for Flow Through Cracks in Pipes, to be presented at the 24th ASME/AICHE National Heat Transfer Conference, Pittsburgh, Pennsylvania, August 9-12, 1987.

3. B. Chexal & J. Horowitz, "A Crack Flow Rate Model for Leak - Before - Break Applications," SMART-9 Transachoir Vol. G, pp. 281-285 (1987).

5. Collier, R.P., et al, "Two Phase Flow Through Interganular Stress Corrosion Cracks and Resulting Acoustic Emmision," EPRI Report No. NP-3540-LD, April 1984.

6. Moody, F.J., "Maximum Two-Phase Vessel Blowdown from Pipes," J. Heat Transfer, Vol. 88, No. 3, 1966, pp. 285-295.

7. Daughterly, R.L. and Franzini, J.B., "Fluid Mechanics with Engineering Applications," McGraw-Hill Book Company, New York 1965.

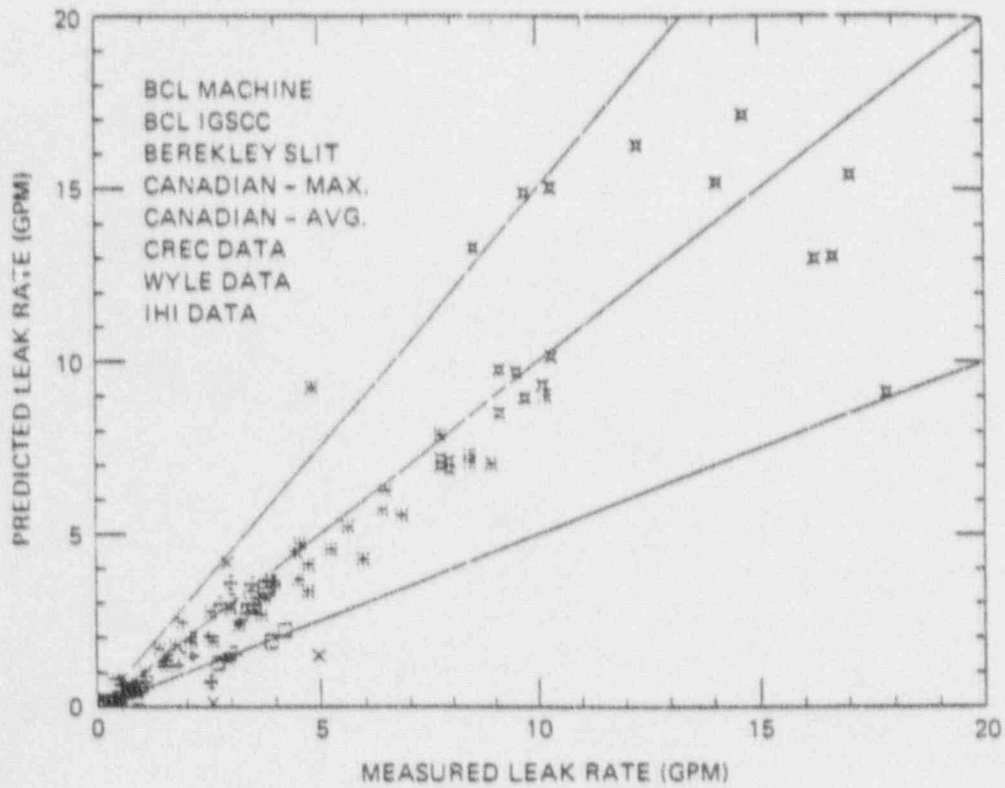
8. P.C. Paris and H. Tada, "The Application of Fracture Proof Design Postulating Circumferential Through-Wall Cracks," U.S Nuclear Regulatory Commission Report NUREG/CR-3464, Washington, DC, April 1983.

4. "Evaluation and Refinement of Leak Rate Estimation Models," NUREG/CR-5128, April 1991.

TABLE 3E.4-1

MASS FLOW RATE FOR SEVERAL Γ/D_h VALUES

Γ/D_h	MASS FLOW RATE, lbm/sec-ft. ² M
0	3800
1	2200
2	1600
3	1150
4	920
5	800
10	580
20	400
50	260
100	185



87-592-21

Figure 3E.4-1 COMPARISON OF PICEP PREDICTIONS WITH MEASURED LEAK RATES

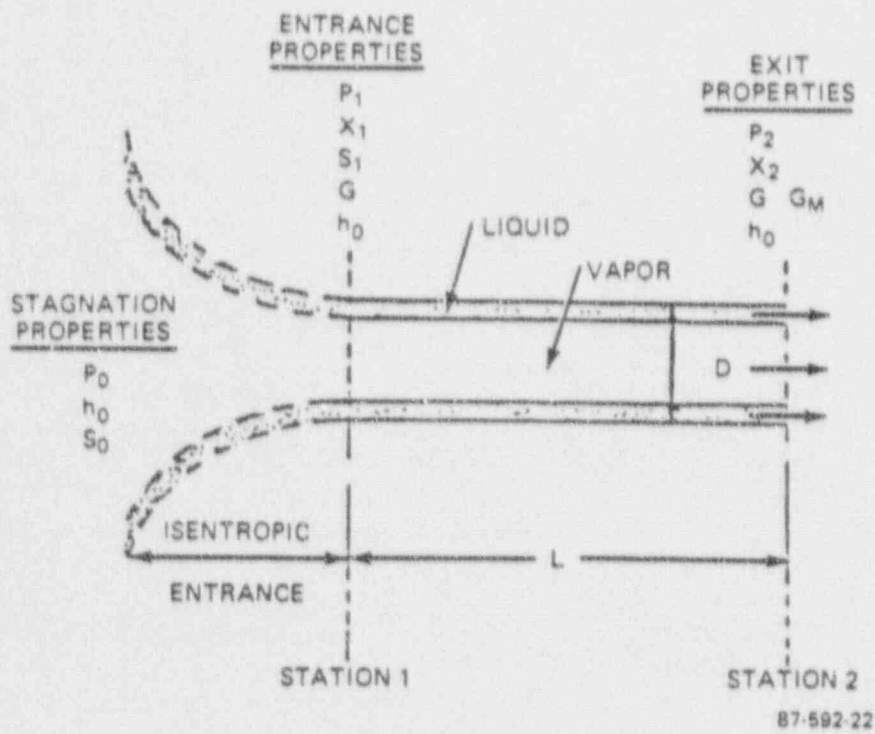
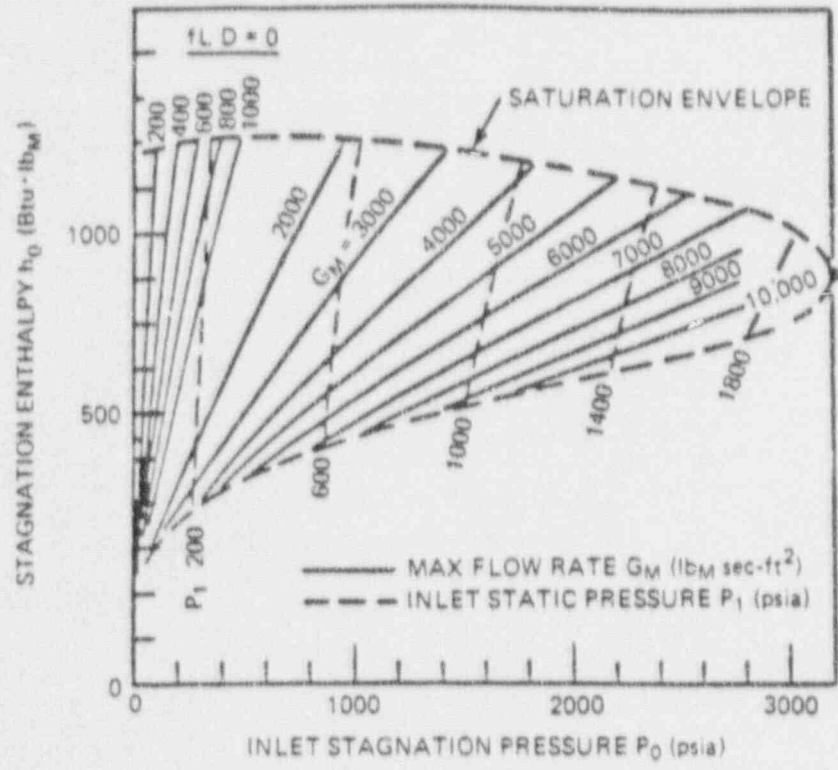
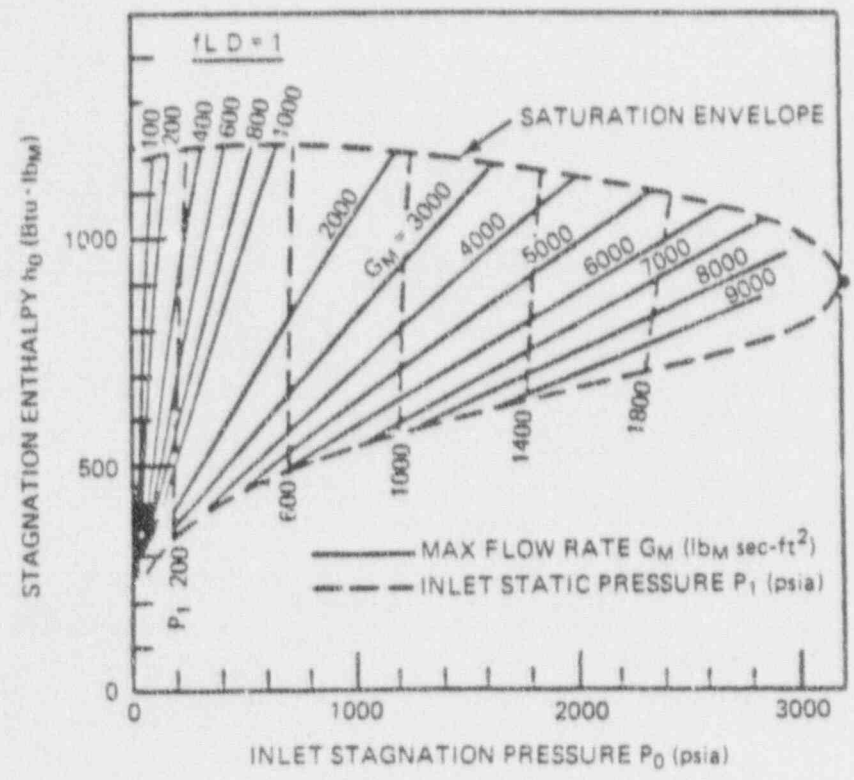


Figure 3E.4-2 PIPE FLOW MODEL



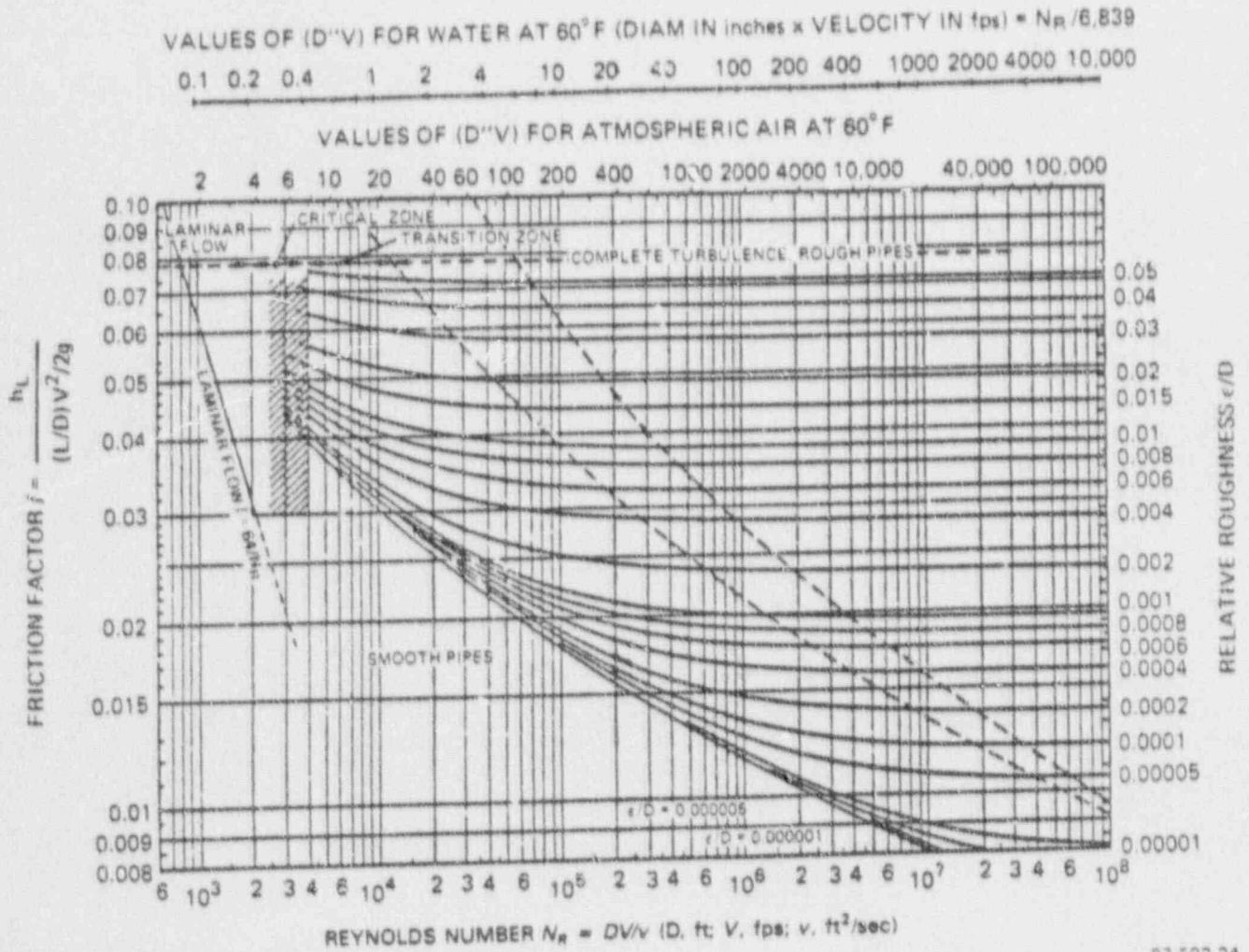
(a)



(b)

87-592-23

Figure 3E.4-3 MASS FLOW RATES FOR STEAM/WATER MIXTURES



87 592-24

Figure 3E.4-4 FRICTION FACTORS FOR PIPES

3E.5 LEAK DETECTION CAPABILITIES

A complete description of various leak detection systems is provided in Subsection 5.2.5. The leakage detection system gives separate considerations to: leakage within the drywell and leakage external to the drywell. The limits for reactor coolant leakage are described in Subsection 5.2.5.4.

The total leakage ^{in the drywell} consists of the identified leakage and the unidentified leakage. The identified leakage is that from pumps, valve stem packings, reactor vessel head seal and other seals, which all discharge to the equipment drain sump. The technical specification limit on the total reactor coolant leakage rate is 25 gpm.

~~The unidentified leak rate is the portion of the total leakage received in the drywell sumps that is not identified as previously described. The licensing (technical specification) limit on unidentified leak rate is 1 gpm. To cover uncertainties in leak detection capability, leak rates of 5 and 10 gpm are used in the leakage flaw size calculations performed in Appendix 3F to evaluate the margins against unstable flaw size and tearing instability load.~~

The unidentified leak rate in the drywell is the portion of the total leakage received in the drywell sumps that is not identified as previously described. The licensing (technical specification) limit on unidentified leak rate is 1 gpm. To cover uncertainties in leak detection capability, although it meets Regulatory Guide 1.45 requirements, a margin factor of 10 is required per Reference 16 of Subsection 3E.3.4 to determine a reference leak rate. A reduced margin factor may be used if accounts can be made of effects of sources of uncertainties such as plugging of the leakage crack with particulate material over time, leakage prediction, measurement techniques, personnel and frequency of monitoring. For the piping in drywell, a reference leak rate of 10 gpm may be used, unless a smaller rate can be justified.

The sensitivity and reliability of leakage detection systems used outside the drywell must be demonstrated to be equivalent to Regulatory Guide 1.45 systems. Methods that have been shown to be acceptable include local leak detection, for example, visual observation or instrumentation. Outside the drywell, the leakage rate detection and the margin factor depend upon the design of the leakage detection systems.

SECTION 3E.6

CONTENTS

<u>Section</u>	<u>Title</u>	<u>Page</u>
3E.6.1	Main Steam Piping Example	3E.6-2
3E.6.2	Feedwater Piping Example	3E.6-6

TABLES

<u>Table</u>	<u>Title</u>	<u>Page</u>
3E.6-1	Stresses in The Main Steam Lines (Assumed for Example)	3E.6-8
3E.6-2	Critical Crack Length and Instability Load Margin Evaluation For Main Steam Lines (Example)	3E.6-8
3E.6-3	Data For Feedwater System Piping (Example)	3E.6-9
3E.6-4	Stresses in Feedwater Lines (Assumed for Example)	3E.6-9
3E.6-5	Critical Crack Length and Instability Load Margin Evaluations For Feedwater Lines (Example)	3E.6-10

ILLUSTRATIONS

<u>Figure</u>	<u>Title</u>	<u>Page</u>
3E.6-1	Leak Rate As a Function Of Crack Length in Main Steam Pipe (Example)	3E.6-11

3E.6 GUIDELINES FOR PREPARATION OF AN LBB REPORT

Some of the key elements of an LBB evaluation report for a high energy piping system are: system description, evaluation of susceptibility to water hammer and thermal fatigue, material specification, piping geometry, stresses and the LBB margin evaluation results. Two examples are presented in the following subsections to provide guidelines and illustration for preparing an LBB evaluation report.

3E.6.1 Main Steam Piping Example

3E.6.1.1 System Description

-- Continued next page --

ABWR Standard Plant

3E.6.1

3E.2 MAIN STEAM PIPING EXAMPLE

3E.6.1.1

3E.2.1 System Description

28-inch (700 mm)

connects to

The four main steam (MS) lines carry steam from the reactor to the turbine and auxiliary systems. The reactor coolant pressure boundary portion of each line being evaluated in this section includes a flow restrictor, which is designed to limit the rate of escaping steam from the postulated break in the downstream steam line. The restrictor is also used for flow measurements during plant operation. The safety relief valves (SRVs) discharge into the pressure suppression pool through SRV discharge piping. The SRV safety function includes protection against over pressure of the reactor primary system. The main steam line A has a branch connection to supply steam to the reactor core isolation cooling (RCIC) system turbine.

reactor building

This section addresses the MS piping system in the ~~nuclear island~~ which is designed and constructed to the requirements of the ASME Code, Section III, Class 1 piping (within outermost isolation valve) and Class 2 piping. It is classified as Seismic Category I. It is inspected according to ASME Code Section XI.

3E.6.1.2

3E.2.2 Susceptibility to Water Hammer

Significant pressure pulsation of water hammer effect in the pipe may occur as a result of opening of SRVs or closing of the turbine stop valve. A brief description of these phenomena follows. These two transients are considered in the main steam piping system design and fatigue analysis. These events are more severe than the opening or closing of a main steam isolation valve or water carry over through main steam and SRV piping. Moreover, the probability of water carry over during core flooding in case of an accident is low.

3E.2.2.1 Safety Relief Valve Lift Transient Description

SRV produces momentary unbalanced forces acting on the discharge piping system for the period from the opening of the SRV until a steady discharge flow from the reactor pressure vessel to the suppression pool is established. This period includes clearing of the water slug at the

a part of the reactor pressure vessel nozzle and is

23A6100AE

REV B

end of the discharge piping submerged in the suppression pool. Pressure waves traveling through the discharge piping following the relatively rapid opening of the SRVs causes the discharge piping to vibrate. This in turn produces time dependent forces that act on the main steam piping segments.

There are a number of events/transients/postulated accidents that result in SRV lift:

- Automatic opening signal when main steam system pressure exceeds the set point for a given valve (there are different set points for different valves in a given plant).
- Automatic opening signal for all valves assigned to the automatic depressurization system function on receipt of proper actuation signal.
- Manual opening signal to valve selected by plant operator.

The SRVs close when the main steam system pressure reaches the relief mode reseal pressure or when the plant operator manually releases the opening signals.

It is assumed (for conservatism) that all SRVs are activated at the same time, which produces simultaneous forces on the main steam piping system.

3E.2.2.2 Turbine Stop Valve Closure Transient Description

Prior to turbine stop valve closure, saturated steam flows through each main steam line at nuclear boiler rated pressure and mass flow rate. Upon signal, the turbine stop valves close rapidly and the steam flow stops at the upstream side of these valves. A pressure wave is created and travels at sonic velocity toward the reactor vessel through each main steam line. The flow of steam into each main steam line from the reactor vessel continues until the fluid compression wave reaches the reactor vessel nozzle. Repeated reflection of the pressure wave at the reactor vessel and stop valve ends of the main steam lines produces time varying pressures and velocities at each point along the main steam

lines. The combination of fluid momentum changes, shear forces, and pressure differences cause forcing functions which vary with position and time to act on the main steam piping system. The fluid transient loads due to turbine stop valve closure is considered as design load for upset condition.

3E.6.1.2 Basic Fluid Transient Concept

Despite the fact that the SRV discharge and the turbine stop valve closure are flow-starting and flow-stopping processes, respectively, the concepts of mass, momentum, and energy conservation and the differential equations which represent these concepts are similar for both problems. The particular solution for either of the problems is obtained by incorporating the appropriate initial conditions and boundary conditions into the basic equations. Thus, relief valve discharge and turbine stop valve closure are seen to be specific solutions of the more general problem of compressible, non-steady fluid flow in a pipe.

The basic fluid dynamic equations which are applicable to both relief valve discharge and turbine stop valve closure are used with the particular fluid boundary conditions of these occurrences. Step-wise solution of these equations generates a time-history of fluid properties at numerous locations along the pipe. Simultaneously, reaction loads on the pipe are determined at each location corresponding to the position of an elbow.

The computer programs RVFOR and TSFOR described in Appendix 3D are used to calculate the fluid transient forces on the piping system due to safety relief valve discharge and turbine stop valve closure. Both of the programs use method of characteristics to calculate the fluid transients.

The results from the RVFOR program have been verified with various inplant test measurements such as from the Monticello tests and Caorso tests and the test sponsored by BWR owner for NUREG-0737 at Wyle test facilities, Huntsville, Alabama. Various data from the strain gages on the pipes and the load cells on the supports were compared with the analytical data and found to be in good correlation.

Evaluation of the ensuing effects are considered as a normal design process for the main steam piping system. The peak pressure pulses are within the design capability of a typical piping design and the piping stresses and support loads remain within the ASME Code allowables.

It is concluded that, during these water hammer type events, the peak pressures and segment loads would not cause overstressed conditions for the main steam piping system.

3E.6.1.3

3E.6.1.3 Thermal Fatigue

No thermal stratification and thermal fatigue are expected in the main steam piping since there is no large source of cold water in these loops. A small amount of water may collect in the near horizontal leg of the main steam line due to steam condensation. However, a slope of 1/8 inch per foot of main steam piping is provided in each main steam line. Water drain lines are provided at the end of slope to drain out the condensate. Thus, in this case no significant thermal cycling effects on the main steam piping are expected.

3E.6.1.4

3E.6.1.4 Piping, Fittings and Safe End Materials

The material specified for the 28-inch main steam pipe is SA155 KCF70. The corresponding specification for the piping fittings and forgings are given as SA420, WPL6 and SA350, LF2, respectively. The material for the safe end forging welded between the main steam piping and the steam nozzle is SA508 Class 3.

3E.6.1.5

3E.6.1.5 LBB Margin Evaluation

The Code stress analysis of the piping will be reviewed to obtain representative stress magnitudes. For the LBB evaluation purpose only one pipe size, i.e., 28-inch, will be considered. Table 3E.6.1 shows the example stress magnitude due to pressure, weight, thermal expansion and SSE loads. 3E.6-1
is
to present

The leak rate calculations were performed assuming saturated steam conditions at 1050 psi. The leak rate model for saturated steam developed in Section 3E.4.2 was used in this may be

evaluation. Pressure, weight and thermal expansion stresses were included in calculating the crack opening area. A plot of leak rate as a function of crack size was developed and is shown in Figure 3E.2-1. Leakage flow lengths corresponding to 5 and 10 gpm were determined from this figure. *the reference leak rate (see section 3E.5) is*

3E.6-1

The calculations for the critical flaw size and instability load corresponding to leakage-size cracks were performed using the J-T methodology. Specifically, the 550°F J-R curve shown in Figure 3E.2-8 and the Ramberg-Osgood parameters given in Subsection 3E.3.2.1 were used. A plot of instability tension and bending stresses as a function of crack length was developed. Table 3E.2-2 shows the calculated critical crack size and the margin along with the instability load margin for the leakage size cracks. It is noted that the critical crack size margin is greater than 2 and the instability load margin also exceeds $\sqrt{2}$.

3E.6-2

example presentation of

3E.6.1.6

3E.2.6 Conclusion

~~For all four loops of the main steam system, leakage rates of 5 and 10 gpm are used in the LBB evaluation based on the limit of satisfactory detection of the associated unidentified leakage. Based upon these leakage rates and representative stress magnitudes, leakage flow lengths are calculated for 28 inch pipe and compared against the critical flaw length. The margin is shown to be greater than 2 for both leakage rates. Also, the leak-size crack stability evaluation showed a margin of at least $\sqrt{2}$.~~

*Continued
next page*

~~It is also shown that other LBB criteria of Section 3.6.3 including immunity to failure from effects of IGSCC, water hammer and thermal fatigue, and capability for leak detection are satisfied. Therefore, all four loops of the main steam piping qualify for the leak-before-break postulation approach.~~

3E.6.1.6 Conclusion

For all main steam lines, based upon the reference leakage rates and assumed stress magnitudes, leakage flaw lengths are calculated and compared against the critical flaw length. The margin is shown to be greater than 2 for the leakage rates. Also, the leak-size crack stability evaluation is shown to have a margin of at least $\sqrt{2}$.

It is also shown that the conditions required for applicability of LBB (see Subsection 3.6.3.2), such as high resistance to failure from effects of IGSCC, water hammer and thermal fatigue, are satisfied. Therefore, all four of the main steam lines qualify for LBB behavior.

3E.6.2
3F.3 FEEDWATER SYSTEM PIPING

EXAMPLE

3E.6.2.1
3F.3.1 System Description

The function of the feedwater (FW) system is to conduct water to the reactor vessel over the full range of the reactor power operation. The feedwater piping consists of two 22-inch diameter lines from the high-pressure feedwater heaters, connecting to the reactor vessel through three 13-inch risers on each line. Each line has one check valve inside the containment drywell and one positive closing check valve outside containment. During shutdown cooling mode, reactor water pumped through the RHR heat exchanger in one loop is returned to the vessel by way of one feedwater line.

each
2
(300 mm)

temperatures, pressures and thickness for representative pipe sizes in the feedwater system. The nominal thickness for both pipe sizes correspond to schedule 80. Table 3F.3.2 shows the present stress magnitudes for each pipe size due to pressure, weight, thermal expansion and SSE loads. Only the pressure weight and thermal expansion stresses are used in the leak rate evaluation, where a sum of all stresses is used in the instability load and critical flaw evaluation.

example
3E.6-4
example
to

3F.3.6 LBB Margin Evaluation

The incoming water of the feedwater system is in a subcooled state. Accordingly, the leakage flow length calculations were based on the procedure outlined in Section 3E.4.1. The saturation pressure, P_{sat} , for each pipe size was calculated from the normal operation temperatures given in Table 3F.3.4. The leak rates were calculated as a function of crack length. The leakage flow lengths corresponding to 5 and 10 gpm leak rates were then determined.

may be
may be
3E.6-3

This section addresses the feedwater piping in the nuclear island, extending from the vessel out to the outboard isolation valve (ASME Class 1) and further through the shutoff valve to and including the seismic interface restraint (ASME Class 2). This section of the feedwater piping is classified as Seismic Category 1.

3E.6.2.2
3F.3.2 Susceptibility to Water Hammer

There is no record of feedwater piping failure due to water hammer. Although there are several check valves in the feedwater system, operating procedure and the control systems have been designed to limit the magnitude of water hammer load to the extent that a formal design is not required.

The calculations for the critical flaw size and the instability load corresponding to leakage size cracks were performed using the J-T methodology. Specifically, the J-T curve shown in Figure 3E.2-9 and the Ramberg-Osgood parameters given in Subsection 3E.3.2.2 were used. Table 3F.3.3 shows the calculated critical crack sizes, and the margins along with the instability load margins for the leakage size cracks. Results are shown for both the 22-inch and 12-inch lines. It is noted that for the two reference leak rates, the critical crack size margin is greater than 2 and the instability load margin also exceeds $\sqrt{2}$.

may be
3E.6-5

3E.6.2.3
3F.3.3 Thermal Fatigue

Thermal fatigue is not a concern in ABWR feedwater piping. The ASME Code evaluation includes operating temperature transients, cold and hot water mixing and thermal stratification.

3E.6.2.7
3F.3.7 Conclusion

LBB evaluation has been conducted using two values of reference leak rates, 5 and 10 gpm. Based upon these leakage rates and representative stress magnitudes, leakage flow lengths were calculated for 22-inch and 12-inch lines. Comparison with critical crack lengths showed margin to be greater than 2. Leakage size crack stability evaluation showed a margin of at least $\sqrt{2}$.

3E.6.2.4
3F.3.4 Pippings, Fittings and Safe End Material

The material for piping is either SA333, Gr. 6, or SA-672, Gr. C70.

3E.6.2.5
3F.3.5 Piping Sizes, Geometries and Representative Stresses

Table 3F.3.1 shows the normal operating

It has been also demonstrated in the

3E.6-3

Sub

preceding subsections that the feedwater line meets other LBB Criteria of Section 3.6.3.2 including immunity to failure from effects of IGSCC, water hammer and thermal fatigue.

3E.6-1
TABLE 3F.2-1

REPRESENTATIVE STRESSES IN THE MAIN STEAM LINES
(ASSUMED FOR EXAMPLE)

Nominal Pipe Size (in)	Pipe O.D. (in)	Nominal Thickness (in)	Long. Pressure Stress (ksi)	Weight + Thermal Expansion Stress (ksi)	SSE Stress (ksi)
28	28.0	1.32	5.17	3.0	5.0

3E.6-2
TABLE 3F.2-2

CRITICAL CRACK LENGTH AND INSTABILITY LOAD MARGIN
EVALUATIONS FOR MAIN STEAM LINES (EXAMPLE)

Pipe Size (in)	Reference Leak Rate (gpm)	Reference Crack Length (in)	Critical Crack Length (in)	Instability ¹ Bending Stress, S _b (ksi)	Margins on	
					Critical Crack	Load ² at Leakage Crack
28	5	11.1	30.7	27.4	2.8	2.5 ^c
28	10 ³	13.45	30.7	24.4	2.3	2.2

NOTES:

1. Based on Equation 3E.3-9a.
2. Based on Equation 3E.3-9b.
3. See subsection 3E.5.

3E.6-3
TABLE 3F-3-1
PIPING (EXAMPLE)
DATA FOR FEEDWATER SYSTEM REPRESENTATION PIPE SIZE

Nominal Pipe Size (in)	Pipe O.D (in)	Nominal Thickness (in)	Nominal Temperature (°F)	Operating Pressure (psig)
12	12.75	0.687	420	1100
22	22.0	1.031	420	1100

3E.6-4
TABLE 3F-3-2

REPRESENTATIVE STRESSES IN FEEDWATER LINES
(ASSUMED FOR EXAMPLE)

Nominal Pipe Size	Longitudinal Pressure Stress (ksi)	Weight + Thermal Expansion Stress (ksi)	Safe Shut-down Earthquake (SSE) Stress (ksi)
12	5.1	4.0	5.0
22	5.4	4.0	5.0

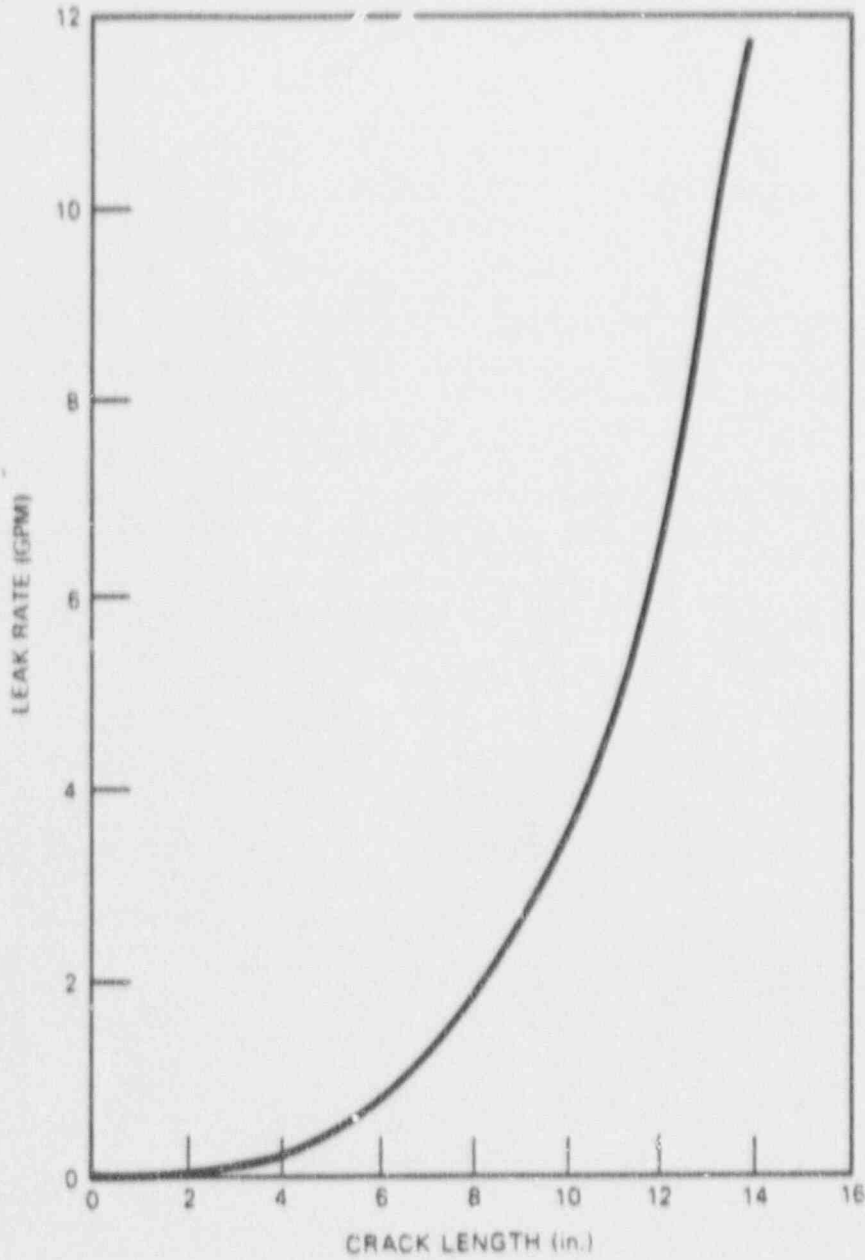
3E.6-5
TABLE 3F.3-3_σ

CRITICAL CRACK LENGTH AND INSTABILITY LOAD MARGIN
EVALUATIONS FOR FEEDWATER LINES (EXAMPLE)

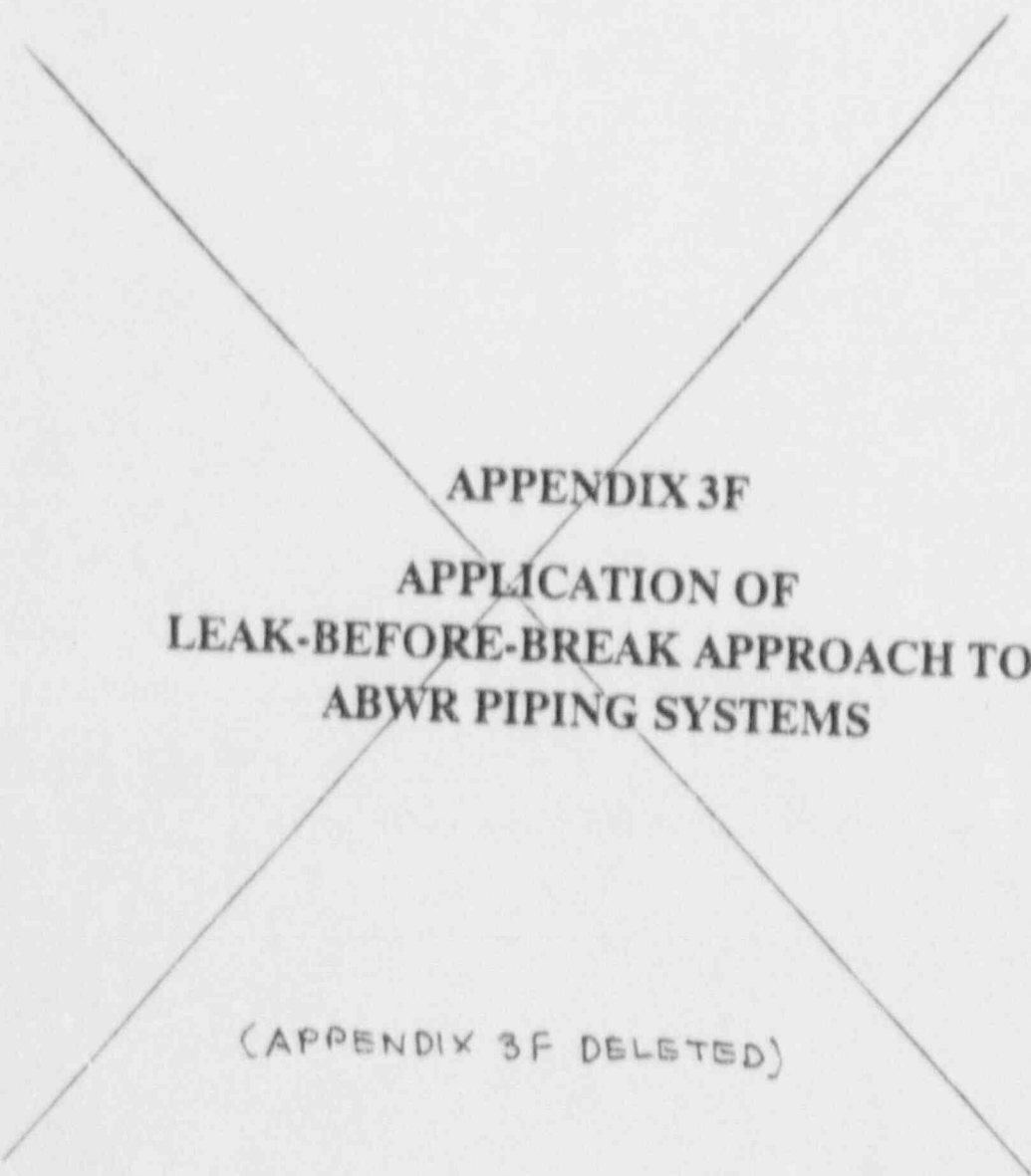
Pipe Size (in)	Reference Leak Rate (gpm)	Reference Crack Length (in)	Critical Crack Length (in)	Instability ¹ Bending Stress, S _b (ksi)	Margins on	
					Critical Crack	Load ² at Leakage Crack
12	5 ³	4.5	13.1	27.2	2.9	2.3 ✓
12	10 ³	5.7	13.1	24.0	2.3	2.1
22	5 ³	5.2	20.4	27.9	3.9	2.3 ✓
22	10 ³	6.7	20.4	25.6	3.1	2.2

NOTES:

1. Based on Equation 3E.3-9a.
2. Based on Equation 3E.3-9b.
3. See Subsection 3E.5.



3E-6-1
Figure 3F-2-5 } LEAK RATE AS A FUNCTION OF CRACK LENGTH
IN MAIN STEAM PIPE (EXAMPLE)



APPENDIX 3F
APPLICATION OF
LEAK-BEFORE-BREAK APPROACH TO
ABWR PIPING SYSTEMS

(APPENDIX 3F DELETED)